energies

MDPI

Review

Challenges in Petroleum Characterization—A Review

Ivelina Shishkova [1], Dicho Stratiev [1,2,*], Iliyan Venkov Kolev [1], Svetoslav Nenov [3], Dimitar Nedanovski [4], Krassimir Atanassov [2], Vitaly Ivanov [5] and Simeon Ribagin [2]

1 LUKOIL Neftohim Burgas, 8104 Burgas, Bulgaria
2 Institute of Biophysics and Biomedical Engineering, Bulgarian Academy of Sciences, Academic GeorgiBonchev 105, 1113 Sofia, Bulgaria
3 Department of Mathematics, University of Chemical Technology and Metallurgy, Kliment Ohridski 8, 1756 Sofia, Bulgaria
4 Faculty of Mathematics and Informatics, "St. Kliment Ohridski" University, 15 Tsar Osvoboditel Blvd., 1504 Sofia, Bulgaria
5 Department of Industrial Technologies and Management, University Prof. Dr. Assen Zlatarov, Professor Yakimov 1, 8010 Burgas, Bulgaria
* Correspondence: stratiev.dicho@neftochim.bg

Abstract: 252 literature sources and about 5000 crude oil assays were reviewed in this work. The review has shown that the petroleum characterization can be classified in three categories: crude oil assay; SARA characterization; and molecular characterization. It was found that the range of petroleum property variation is so wide that the same crude oil property cannot be measured by the use of a single standard method. To the best of our knowledge for the first time the application of the additive rule to predict crude oil asphaltene content from that of the vacuum residue multiplied by the vacuum residue TBP yield was examined. It was also discovered that a strong linear relation between the contents of C_5-, and C_7-asphaltenes in crude oil and derived thereof vacuum residue fraction exists. The six parameter Weibull extreme function showed to best fit the TBP data of all crude oil types, allowing construction of a correct TBP curve and detection of measurement errors. A new SARA reconstitution approach is proposed to overcome the poor SARA analysis mass balance when crude oils with lower density are analyzed. The use of a chemometric approach with combination of spectroscopic data was found very helpful in extracting information about the composition of complex petroleum matrices consisting of a large number of components.

Keywords: petroleum; crude oil; characterization; SARA; asphaltenes; TBP; modeling; ICrA

Citation: Shishkova, I.; Stratiev, D.; Kolev, I.V.; Nenov, S.; Nedanovski, D.; Atanassov, K.; Ivanov, V.; Ribagin, S. Challenges in Petroleum Characterization—A Review. *Energies* **2022**, *15*, 7765. https://doi.org/10.3390/en15207765

Academic Editor: Hemanta Sarma

Received: 21 September 2022
Accepted: 17 October 2022
Published: 20 October 2022

1. Introduction

The petroleum is a mineral consisting of myriad hydrocarbons and sulfur, oxygen, nitrogen, and metal containing organic species with diverse composition, structure and molecular weight [1,2]. Although it is not considered as a renewable source its extinguishing has been deemed in the past to be finished nowadays. However, the continual discovering of new oil fields over the years continually move the expected time in the future when the petroleum crude as a mineral source is to be extinguished [2]. In order to rationalize the petroleum crude usage, one needs to know its chemical nature. That is not an easy task because the crude oil is made up of a myriad of organic substances with different composition, structure, and molecular weight [3,4]. The distribution of the petroleum properties such as density, molecular weight, H/C ratio and others can be described by probability distribution functions [5–7]. The processes employed to manufacture different petroleum derived products such as fuels, monomers, feeds for the organic synthesis, and polymers are found to strongly depend on the characteristics of the petroleum feedstock [8,9]. That is why the characterization of the petroleum crudes takes a pivotal place in many studies [10–25]. Many different techniques have been applied to investigate the chemical nature of the different crude oils explored around the world. Although the

tremendous advance in the sophisticated analytical methods used to characterize the most difficult part of the petroleum crude: so called "bottom of the barrel", and its most difficult to analyze and understand part—the asphaltenes or heptane/pentane insolubles the mutual relations of the different compounds making up the petroleum are still not well understood [26].

Petroleum is not a uniform crude material. Each petroleum crude produced in the world has a sui generis chemical constitution, which fluctuates depending on the manner of its formation. Typically, more than 150 crude grades are traded [27] worldwide, and many of these traded crude oils are obtained by blending petroleum crudes from two or more fields. There is a very big variation in the properties of the petroleum crudes around the world which will be discussed later in this review article. Oil refining is a process of transforming of crude oil into marketable products such as fuels, lubricants, and light olefins-feeds for the petrochemical industry. The stringent environmental regulations, the strict refining product specifications along with the limited availability of light sweet crude oils, and the volatile refining margins shrank the number of the operating refineries worldwide from about 750 to 643 for a period of 12 years [8]. The shift of product demand from fuels to light olefins is another challenge the oil refining is facing [28]. All changes occurring in the petroleum refining a result from the ever-increasing stringent environmental regulations, new tougher product specifications, the searched outlet for processing of waste and biomaterials [29] together with the natural requirement for any business process to be profitable demand adopting innovative techniques. The purchasing of crude oil is the largest cost in oil refining (Figure 1) and its share among all refining costs has increased from 80% [30] up to 95% [31] over the years. Therefore, processing of cheaper crude oils, also called "opportunity crudes" (OCs), or "advantages oils" could improve the oil refining profitability [2]. However, the OCs are cheaper because of their lower quality and their processing presents extraordinary technical challenges [2]. The OCs contain higher amount of harmful for the refining processes compounds such as asphaltenes, metal-bearing species, and naphthenic acids, which jeopardize the smooth operation of the refinery [2]. Their physical properties and reactivity have severe consequences in oil refining [2]. A lack of comprehensive knowledge of these molecules may cause an unplanned shut down for cleaning or repairing of refining process equipment leading to a huge loss of profit opportunity when OCs are processed. In order to comprehend better the features of OCs and their impact on refining process performance investigations are needed which, unfortunately are expensive. A comprehensive laboratory crude oil assay may cost in excess of 20,000 USD [32].

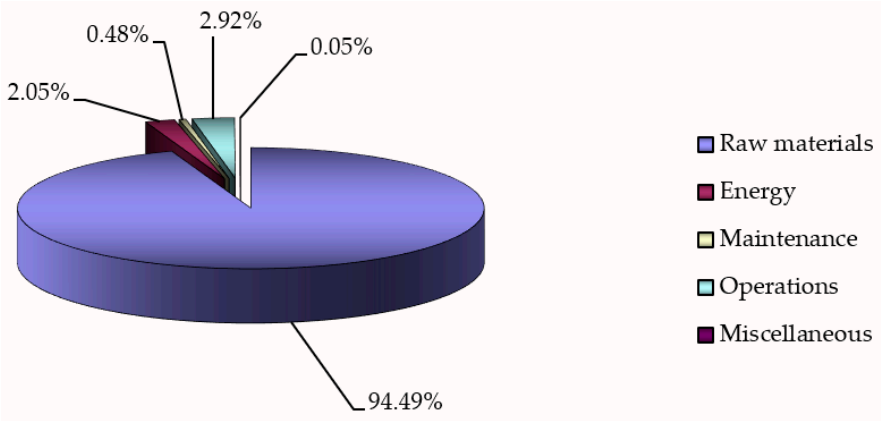

Figure 1. Structure of costs in a modern oil refinery.

Only a small number of major oil companies have the resources to produce in-house library of laboratory assays for crude oils around the world [32]. It is difficult even with these laboratory crude oil assays in hands to properly predict the behavior of the OCs during their processing because the oil refineries typically process not a single crude but

a blend of crudes [33]. For that reason, properly modeling and prediction of petroleum blend properties is required [34,35]. In this paper we present a comprehensive review of the methods reported in the literature to study the chemistry and technology of petroleum and the challenges researchers overcome during doing this job with the aim to find out the most efficient way to process the different grades of available crude oils around the world and produce products needed to satisfy mankind needs.

2. Petroleum Characterization by Means of Crude Oil Assay

The petroleum characterization by means of crude oil assay consists of performance of several laboratory tests to measure physical and chemical properties of whole crudes and several distilled fractions [11,36–41]. Usually, the boiling ranges of distilled fractions coincide with those of commercial fuels, produced in the refineries [36]. The crude oil assays can be classified as comprehensive (full) and short, or inspection assays. The full assays are ample and particularly significant for new crudes. In a crude assay, analyses are carried out by combination of atmospheric and vacuum distillation tests to generate a true boiling-point (TBP) distillation data. A full assay is obtained from a series of physical and chemical tests that give a precise representation of petroleum quality and petroleum product quality and enable an instruction for its behavior during refining, transportation, or storage [11]. At minimum, the assay should contain a distillation curve, typically a TBP curve, and a specific gravity curve. A typical analysis scheme of petroleum characterization by a comprehensive crude oil assay (full assay) is presented in Figure 2.

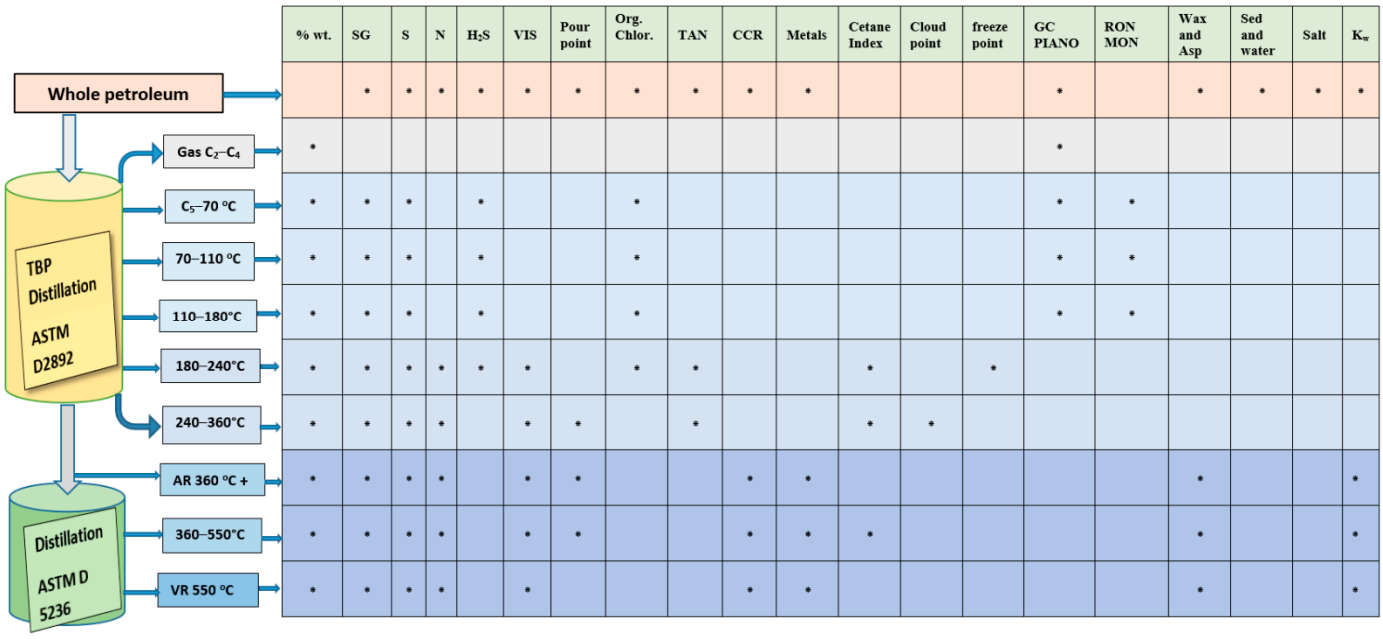

Figure 2. Typical analysis scheme of petroleum characterization by means of crude oil assay. Note: The sign ● means performance of measurement of the property shown in the first row of the table of Figure 2.

The comprehensive assay is complex, costly, and time-consuming and is normally performed only when a new field comes on stream for which a company has an equity interest, a crude that has not previously been processed arrives at a refinery, or when the inspection assay indicates that significant changes in the stream's composition have occurred [37]. The typical comprehensive assays of extra light (API > 40), light (30 < API < 40), medium (20 < API < 30), heavy (10 < API < 20) and heavy-extra heavy crude oils (API ≈ 10) from all over the world are presented in Table S1. It is interesting to note here that crude oils with close density have very different fraction distributions and properties of its distillated derivatives (for example see Table S1: Cinta from Indonesia and Istmust from Mexico; Wilm-

ington from USA and Eocene from Kuwait). Petroleum properties depend on its maturity and geographic region of origin. Petroleum having a gravity below 20°API (heavy crude oils with SG above 0.934) are immature, and those having more than 20°API are mature [42]. In addition, crude oil sulfur content depends on source origin and maturity. Crude oils originating from marine source have sulfur content below 1%, and those originated from non-marine origin have sulfur content above 1% [43]. Crude oil maturity increases with the decrease of sulfur content [44]. The typical minimum assays of extra light, light, medium, and heavy crude oils are presented in Tables S1–S3. The data in Tables S1–S3 includes TBP curve data, and density and sulfur distribution of 37 extra light, light, medium, and heavy crude oils. The cost for performance of a comprehensive crude oil assay as that shown in Table S1 amounts of 11,000 Euro, while that of the short, or so-called inspection assay [37] as that shown in Tables S1–S3 amounts of 5600 Euro (cost level of 2022). The variation of petroleum bulk properties extracted from a great number of available crude oil assays (more than 4000), and from literature sources is summarized in Table 1.

Table 1. Range of variation of bulk properties of crude oils.

	Minimum	**Maximum**
Density at 15 °C (g/cm^3)	0.746 [45]	1.119 [46]
Viscosity at 40 °C	0.54 [45]	10^6 [46]
Pour point (°C)	−40	63
Carbon (%wt)	83 [2]	87 [2]
Hydrogen (%wt)	10 [2]	14 [2]
Sulphur (Total) (%wt)	0.05 [2]	9.0 *
Nitrogen (Total) (%wt)	0.05 [2]	3.0 [2]
Oxygen (Total) (%wt)	0.05 [2]	1.5 [2]
Nickel (ppm wt)	0	237
Vanadium (ppm wt)	0	1200
TAN, mgKOH/100 g	<0.01	5.05 [31]
Molecular weight, g/mol	117 [45]	652 [47]
TBP wide fraction yields, %wt		
30–100 °C (Light naphtha; C_5–C_7)	0	27.4
100–180 °C (Heavy naphtha; C_7–C_{10})	0	62.4
180–240 °C (Kerosene; C_{11}–C_{14})	0	62.6
240–360 °C (Diesel; C_{15}–C_{22})	0	99.7
360–540 °C (vacuum gas oil; C_{23}–C_{46})	0	87.2
>540 °C (vacuum residue; >C_{46})	0	68.2
Group hydrocarbon composition of crude oil		
Saturates (%wt)	4	88.9
Aromatics, (%wt)	3.4	59.6
Resins (%wt)	0	62.6
C_7-asphaltenes, %wt	0	43.0

* Note of Table 1: crude oil Gianna, Italy.

The data in Table 1 indicates that the bulk properties of petroleum crudes can vary in a very wide range. For example, the minimum density of petroleum crude of 0.746 g/cm^3 [45] corresponds to the density of medium naphtha (fr. 100–150 °C) as evident from the data in Table S1. Whereas the maximum density of petroleum crudes of 1.119 g/cm^3 is very close to the density of the heaviest and most polar fraction of the crude oil—asphaltenes [48]. The minimum molecular weight of petroleum crude of 117 g/mol. is within the range of the naphtha fraction [49], while the maximum molecular weight of petroleum crude of 652 g/mol. is within the range of the vacuum residue fraction [26,50]. The range of variation of the properties between the different crude oils can be so wide that in some cases the same property cannot be measured by the use of a single standard method (nitrogen, metals, viscosity, density, etc.) and different approaches are searched to obtain reliable values for the same petroleum property [51–53]. The petroleum maximum content of C_7-asphaltenes of 43.0% [46] is much higher than that of the heaviest, the highest boiling point fraction—vacuum residue of the crude oils displayed in Table S1. The C_7-asphaltenes are

concentrated in the crude oil vacuum residue. The distilled fractions usually do not exhibit presence of C_7-asphaltenes, and therefore one may expect that the crude oil asphaltene content would be equal to the multiplication of the petroleum vacuum residue content and the vacuum residue asphaltene content. However, our recent study indicated that asphaltenes as solubility class petroleum components do not always obey the additive rule [54]. In order to test whether the crude oil asphaltene content can be predicted from the vacuum residue asphaltene content and TBP yield we performed analyses of asphaltene content in both crude oils and derived thereof vacuum residues. We also measured asphaltene content in the lighter than vacuum residue, vacuum gas oil fractions and detected no asphaltene content therein. No published reports were found examining the application of the additive rule to predict crude oil asphaltene content from that of the vacuum residue multiplied by the vacuum residue TBP yield. Table 2 presents data of content of C_5-, and C_7-asphaltenes in 28 crude oils and their vacuum residue fractions and juxtaposes the measured against estimated asphaltene contents using the additive rule (multiplication of the petroleum vacuum residue content by the vacuum residue asphaltene content). Figure 3 exhibits graphs of measured versus estimated C_7- and C_5-asphaltene contents using the additive rule. From this data it could be deduced that the crude asphaltene content could be predicted from the TBP vacuum residue yield multiplied by its asphaltene content. The data in Figure 3 also shows that the measured asphaltene content is in general higher than that of the estimated one, probably because of the poorer solubility power of the crude oil maltene fraction, than that of the vacuum residue maltene fraction. Another interesting finding taken from the data in Table 2 concerning the relation of C_5- to C_7-asphaltenes is depicted in Figure 4. It is evident from this data that the ratio between C_5- and C_7-asphaltenes in both parent crude oils and the derived thereof vacuum residue fractions is the same. This data also shows that if information of the content of C_7-asphaltenes is available then the content of C_5-asphaltenes can be computed from the regression equation shown in Figure 4. Furthermore, the difference between C_5-, and C_7-asphaltenes determines the n-heptane soluble, n-pentane insoluble, that is the n-pentane insoluble resins. In this way in case of available information about saturate content in the crude oil, and C_7-, or C_5-asphaltenes, the full SARA (saturates, aromatics, resins, asphaltenes) composition can be obtained.

Table 2. Content of C_5-, and C_7-asphaltenes in crude oils and their vacuum residue fractions.

Crude Oil	Crude d 15 °C, g/cm^3	Crude Sulphur, %	>540 °C, %wt	VR C_7-asp, %wt	VR C_5-asp, %wt	Estimated C_7-asp.% in Crude Oil	Estimated C_5-asp.% in Crude Oil	Measured C_7-asp.% in Crude Oil	Measured C_5-asp.% in Crude Oil
Urals	0.877	1.53	25.2	14.1	17.6	3.6	4.4	3.8	6.3
Arab Med.	0.872	2.48	25.2	14.6	25.5	3.7	6.4	5.6	8.9
Arab Heavy	0.889	2.91	32	21.3	32.9	6.8	10.5	3.3	5.7
Val'Dagri	0.832	1.97	14.6	8.5	19.5	1.2	2.8	1.9	3.6
Basrah L	0.878	2.85	28.3	18	27.7	5.1	7.8	9.0	11.1
Basrah H	0.905	3.86	33.8	27.7	37	9.4	12.5	9.7	14.8
Kirkuk	0.873	2.65	24.6	24.3	33.1	6.0	8.1	7.0	11.2
KEB	0.876	2.64	27.7	16.6	25.7	4.6	7.1	7.7	11.7
El Bouri	0.891	1.76	26.2	17.5	27.3	4.6	7.2	8.2	11.9
Kazakh H	0.858	0.81	23.7	11.1	17.8	2.6	4.2	3.1	5.8
CPC	0.805	0.63	9.3	3.4	11	0.3	1.0	1.0	2.0
LSCO	0.854	0.57	18.7	7.8	15.5	1.5	2.9	3.2	6.3
Prinos	0.875	3.71	20.3	30	38.8	6.1	7.9	9.1	14.7
SGC	0.883	2.26	30.1	21.8	28.4	6.6	8.5	7.9	13.3
Oryx	0.916	4.21	37.4	30.9	39.6	11.6	14.8	16.5	23.7
Okwuibome	0.868	0.2	6.9	1.7	8.2	0.1	0.6	1.4	1.9
Boscan	1.002	5.5	63.1	35.2	41	22.2	25.9	27.5	37.0
RasGharib	0.926	3.44	40.2	26	34.9	10.5	14.0	17.8	25.5
Albania	1.001	5.64	48.2	37.7	49.7	18.2	24.0	30.8	36.5
Tempa Rossa	0.940	5.35	37.6	36.8	46.8	13.8	17.6	15.6	20.5
Forties	0.817	0.68	11.9	7.2	9.8	0.9	1.2	3.2	4.8
Rhemoura	0.865	0.75	20.2	23.2	31.3	4.7	6.3	6.2	10.3
Cheleken	0.847	0.40	16.6	5.8	12.5	1.0	2.1	2.3	3.2
Arab Light	0.858	1.89	22.9	12.1	18.8	2.8	4.3	4.7	7.6
Azeri Light	0.848	0.2	14.8	1.4	5.4	0.2	0.8	1.1	1.7
Aseng	0.874	0.26	13.8	3.7	10	0.5	1.4	3.0	4.7
Buzachi	0.907	1.57	32.7	1.8	6.1	0.6	2.0	5.1	8.6
KBT	0.876	2.91	25.8	24.9	32.4	6.4	8.4	5.7	8.9

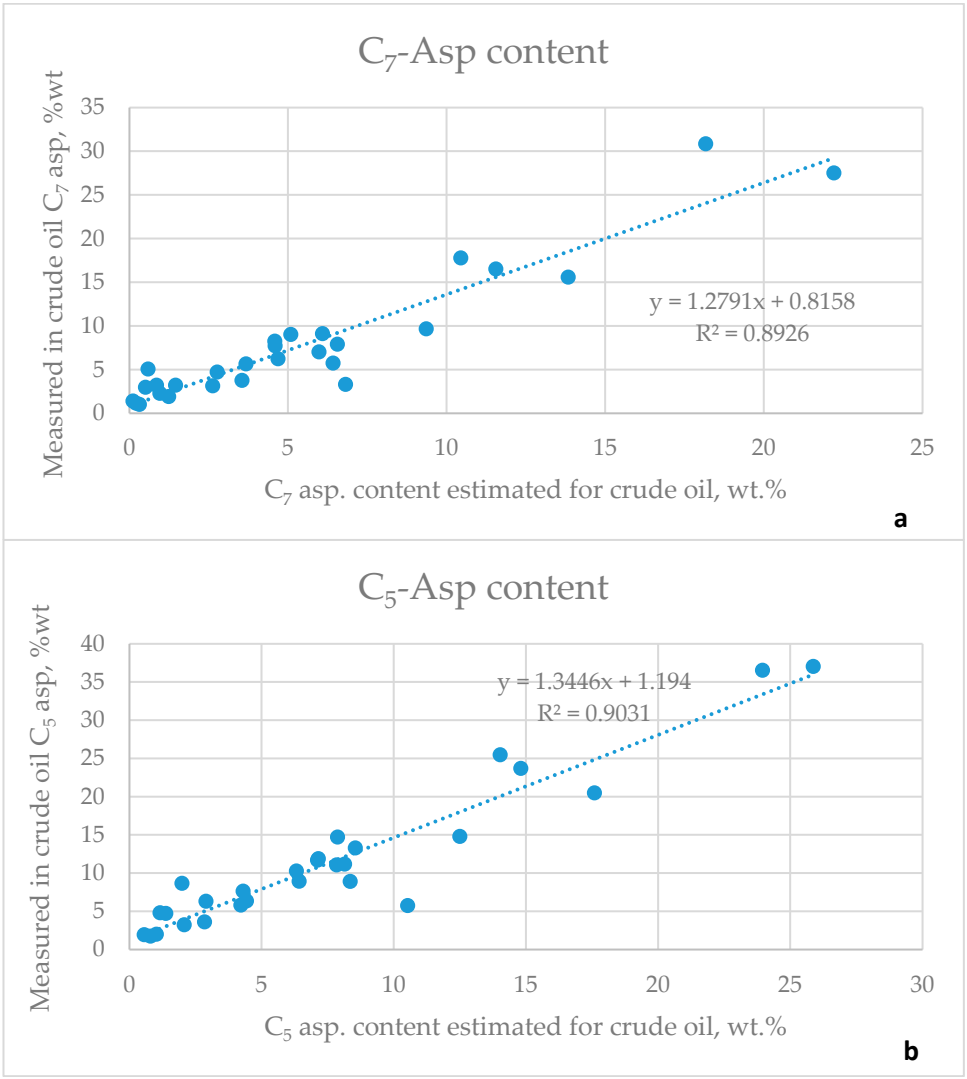

Figure 3. Measured versus estimated C_7- (**a**) and C_5- (**b**) asphaltene contents using the additive rule.

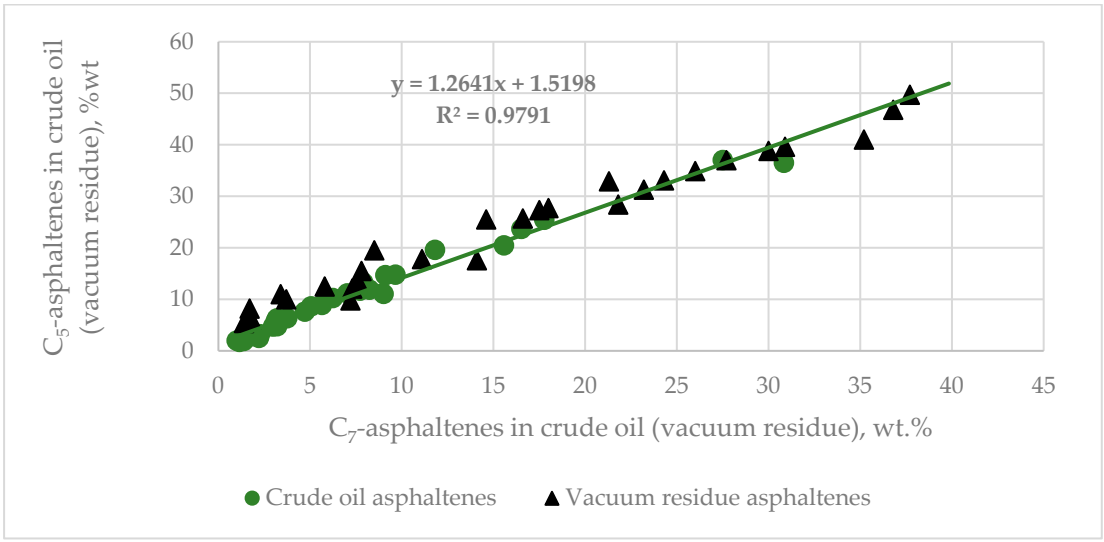

Figure 4. Relation of C_7- to C_5-asphaltenes in crude oils and in their vacuum residue fractions.

The true boiling point (TBP) distillation analysis is the heart of the petroleum crude characterization process because it provides information about the quantity of the different fractions, which are treated in the different refinery plants such as isomerization, reforming, hydrotreatment, fluid catalytic cracking, hydrocracking, etc. [55–90]. It also provides quantity of the different petroleum fractions to be further analyzed for their characteristics (Figure 2) [11,36]. Typically, the crude oil TBP analysis is performed in accordance with the standards ASTM D 2892 (crude oil distillation under atmospheric pressure) and ASTM D 5236 (atmospheric residue distillation under vacuum). The TBP analysis of a crude oil is usually performed for three days. Two days lasts the ASTM D 2892 analysis, and a day is required to complete the ASTM D 5236 analysis. Graphs of the TBP distillation curves of extra light (CPC), light (Azeri Light), medium (Urals), and heavy (RasGharib) crude oils are depicted in Figure 5.

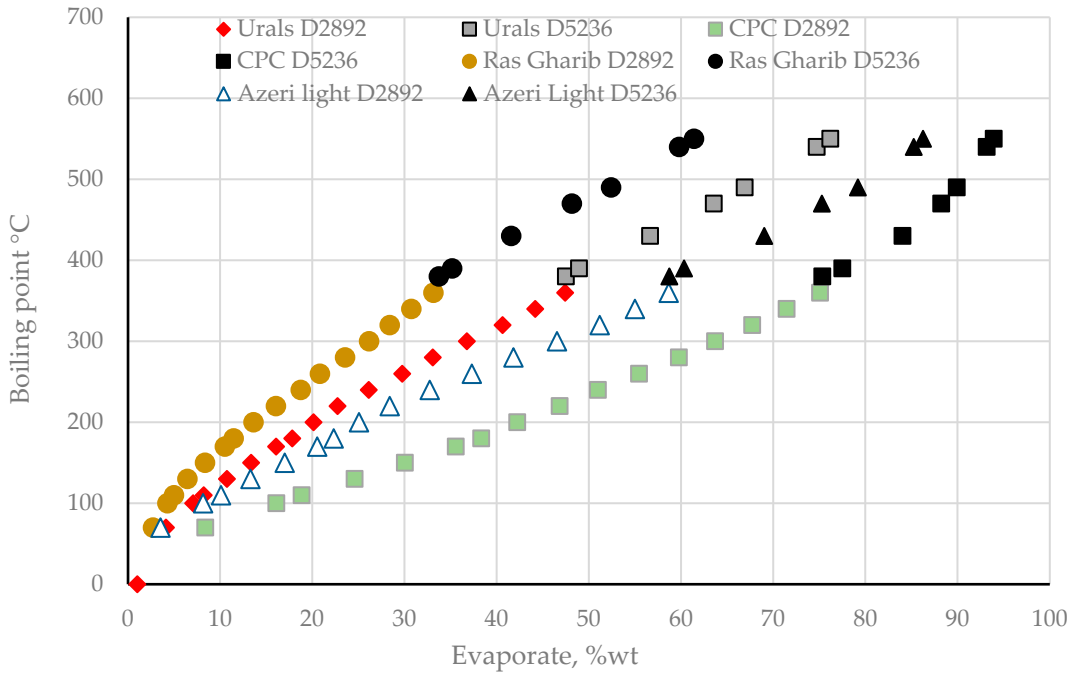

Figure 5. TBP distillation curves using ASTM D 2892 and ASTM D 5236 analysis data for extra light (CPC), light (Azeri Light), medium (Urals), and heavy (RasGharib) crude oils.

One can see from the data in Figure 5 that the points of the distillations ASTM D 2892 and ASTM D 5236 do not lie exactly at the same curve. A shift to higher boiling points at the transition of ASTM D 2892 to ASTM D 5236 is observed. This leads to appearance of a gap in the content of the fraction 360–380 °C that is the first fraction of the ASTM D5236 vacuum distillation, as observed in the data in Table S2. It is difficult to believe that such a gap can physically exist in a continuous distillation curve. Some researchers have employed different interpolation functions to fit distillation curves of petroleum fluids [6,7,17,55,61,62,87–90]. Sanchez et al. [61] concluded that Weibull extreme, Weibull, and Kumaraswamy probability distribution functions are recommended for fitting distillation data. Behrenbruch, and Dedigama [62] employed a two-parameter form of gamma distribution function to fit TBP distillation of 24 extra light, light, medium, and heavy crude oils. Xavier et al. [88] studied TBP distillation data (ASTM D 5307 and ASTM D 2892) of 41 Brazilian crude oils and availed two parameters Beta, Gamma, Riazi, Weibull and four parametric Weibull extreme distribution functions. Their research confirms the conclusion made by Sanchez et al. [61] that the Weibull extreme model presents the best performance within the models in terms of correlation coefficient and root mean squared error. Kotzakoulakis and George [90] used Riazi's distribution model to fit TBP distillation curve of crude oils. Hosseinifar, and Shahverdi [17,55,89] employed third order polynomial

to fit petroleum fluid distillation data. They reported in their recent study [89] that the third order polynomial outperformed the probability distribution functions Beta, Gamma, Riazi, Weibull and Weibull extreme. In our review article we tested the probability distribution functions: five parametric Weibull (Equation (1)), six parametric Weibull extreme (Equation (2)), four parametric gamma (Equation (3)), four parametric beta (Equation (4)), Riazi's distribution model (Equation (5)), and the third polynomial model as described by Hosseinifar, and Shahverdi in [17,55,89] (Equation (6)).

$$F_1(x) = a_1\left(1 - \exp\left(-\left(\frac{x - a_2}{a_3}\right)^{a_4}\right)\right) + a_5 \quad (1)$$

$$F_2(x) = a_1\left(1 - \exp\left(-\left(\frac{x - a_2}{a_3}\right)^{a_4}\right)\right)^{a_5} + a_6 \quad (2)$$

$$F_3 = a_1\left(1 - \frac{1}{\Gamma_{a_2}}\Gamma(a_2, a_3x + a_4)\right) \quad (3)$$

$$F_4 = a_1\frac{B_{(x,a_2,a_3)}}{B_{(a_2,a_3)}} + a_4 \quad (4)$$

Here $\Gamma(x)$ is the gamma function, $\Gamma(a,x)$ is the incomplete gamma function, B(a,b) is the beta function, B(x,a,b) is the incomplete beta function. In addition, a_1, a_2, a_3, a_4, a_5, a_6 are parameters which must be statistically fitted to experimental data.

$$\frac{T_i - T_0}{T_0} = \left[\frac{A}{B}Ln\left(\frac{1}{1 - x_i}\right)\right]^{\frac{1}{B}} \quad (5)$$

$$T_d(x_v) = Ax_v^3 + Bx_v^2 + Cx_v + D \quad (6)$$

These mathematical functions were used to simulate the TBP boiling point distributions of the crude oils from Table S2. Table 3 summarizes the average absolute error of prediction of evaporate yield at different boiling points for the studied crude oils. It is evident from this data that the order of increasing error in predicting the evaporate yield at a definite boiling point is following: Weibul (%AAD = 7.11) > Third polynomial (%AAD = 3.44) > Riazi's distribution model (%AAD = 0.73) > Gamma (%AAD = 0.65) > Beta (%AAD = 0.58) > Weibull extreme (%AAD = 0.51). Thus, the six parameter Weibull extreme function outperforms the other boiling point distribution models, and our study is in line with the conclusions made by Sanchez et al. [61], and Xavier et al. [88]. In addition to the use of probability distribution functions help fill the gap between the last ASTM D2892 and the first ASTM D5236 fractions as indicated in the data of Table 4. In this way, the drawback of combining both distillation data ASTM D2892 and ASTM D5236 during construction of the crude oil TBP curve can be overcome using the probability distribution functions. The model distribution functions approximating TBP curves can be also used to verify the correctness of the performed crude TBP analysis. Table 5 presents data of TBP fraction yields of Azeri Light crude oil measured in two different laboratories and estimated refinery margins using the refinery LP model (Honeywell Refinery and Petro-chemistry modeling System (RPMS)) and employing the TBP distillation yields measured in both laboratories. The two TBP fraction yields exhibited a refinery margin difference of 2 million USD/month confusing the refinery management which TBP curve data to use in the process of refinery production planning. As apparent from the data in Table 3 Lab. 1 exhibits a lower error in fitting the TBP distillation data to the model functions than the data from Lab.2 suggesting that the Lab1 data must be more correct. An erroneous TBP analysis may lead to underestimation or overestimation the refinery margin from processing of a particular crude oil and may result in an erroneous crude selection. Thus, the correctness of the TBP analysis is vital for the proper refinery production planning. Unfortunately, the TBP analysis takes too much time and its substitution with other faster distillation methods has been investigated in several studies being the simulated distillation the best

candidate [56,69,74,77,78]. However, as evident from the data presented in Figure 6 there is a different pattern between TBP, and simulated distillation (ASTM D7169) for the different crude oils. The heavy-extra heavy crude oils (Boscan and Albanian) were incapable of analyzing the TBP distillation by ASTM D2892. Instead, they were capable of analyzing by the physical vacuum distillation in accordance with the ASTM D 1160 standard that is considered equivalent to TBP.

Table 3. Average absolute error of prediction of evaporate yield at different boiling points for the studied crude oils.

		Average ab.s Error. %wt					
Nr.	**Crude Oil**	**Weibull**	**Weibull Extreme**	**Gamma**	**Beta**	**Riazi**	**Third Polynomial**
1	Urarls	107.9	0.57	0.57	0.59	0.62	0.93
2	Arab M	0.4	0.44	0.45	0.52	0.52	0.79
3	Arab H	0.6	0.58	0.61	0.66	0.67	0.91
4	Vald	0.4	0.40	0.41	0.49	0.60	2.07
5	Basrah L	0.4	0.40	0.66	0.39	0.85	2.74
6	Basrah H	0.5	0.46	0.52	0.51	0.66	3.14
7	Kirkuk	0.4	0.42	0.44	0.57	0.74	2.43
8	Iran H	56.5	0.71	0.77	0.75	0.75	1.56
9	CPC	0.4	0.45	0.58	0.59	0.61	3.12
10	RasGarib	99.3	0.51	0.54	0.50	0.70	2.20
11	Okwibome	0.9	0.89	2.05	0.99	0.95	9.23
12	Kazakh2	0.3	0.29	0.42	0.39	0.54	0.89
13	LSCO	0.4	0.40	0.41	0.52	0.83	1.30
14	Rhem	0.6	0.52	0.58	0.63	1.02	1.86
15	Prinos	0.6	0.62	0.71	0.62	0.79	1.58
16	Azeri L	0.5	0.76	0.61	4.86	0.74	1.70
17	SGC	0.5	0.49	0.52	0.50	0.70	4.09
18	Oryx	0.1	0.21	0.18	0.12	0.45	2.91
19	Varandey	0.5	0.59	0.64	0.52	0.61	2.32
20	Arab L	0.6	0.65	0.65	0.71	0.70	2.22
21	KBT	0.4	0.45	0.47	0.52	0.54	2.82
22	Tempa Rossa	0.7	0.74	0.74	0.58	0.77	4.02
23	Forties	0.3	0.33	0.39	0.37	1.13	2.43
24	Aseng	0.8	1.16	0.93	0.98	1.64	3.05
25	Kuwait L	0.4	2.32	0.46	0.71	0.47	1.59
26	Cheleken	0.5	0.58	0.79	0.81	0.51	2.63
27	Caspian H	0.7	0.66	1.42	0.75	0.59	2.94
28	Kumkol	0.6	0.77	0.76	0.52	1.04	2.09
29	Bonga	1.0	1.10	1.54	1.18	1.02	4.86
30	KEB	76.4	10.57	0.39	0.45	0.50	2.50
31	El Bouri	0.2	0.20	0.21	0.16	0.60	1.14
32	Forouzan	0.5	0.47	0.51	0.45	0.86	2.85
33	Azeri L (Lab.1)	0.6	0.57	0.59	0.55	0.54	6.38
34	Azeri L (Lab.2)	0.8	0.75	0.91	0.79	1.07	6.29
35	El Sharara	0.4	0.48	27.59	0.63	0.53	16.96
36	Helm	0.6	0.61	0.86	0.60	0.68	10.84
	AVERAGE	7.11	0.51	0.65	0.58	0.73	3.44
	MAX	107.90	0.89	2.05	0.99	1.02	16.96

Table 4. 20 °C fraction yields of crude oil TBP curve close to the boundary 360–380 °C gap fraction.

		ASTM D2892 Fractions, °C/Yields, %wt			ASTM D-5236 Fractions, °C/Yields, %wt		
Nr		**300–320**	**320–340**	**340–360**	**360–380**	**Estimated by Weibull Extreme Model 360–380**	**380–400**
1	Urals	3.83	3.4	3.29	**0.29**	**3.3**	3.3
2	Arab M	3.72	3.22	3.32	**0.21**	**3.1**	3.5
3	Arab H	3.21	3.25	3.11	**0.08**	**3.0**	3.0
4	Val'Dagri	3.64	3.53	3.26	**0.35**	**2.93**	3.1
5	Basrah L	3.16	3.43	3.22	**0.22**	**2.91**	3.0
6	Basrah H	2.81	3.26	2.53	**0.18**	**2.79**	2.8
7	Kirkuk	3.33	3.29	3.25	**0.22**	**2.94**	3.0
8	Iranian H	3.32	3.09	3.07	**0.2**	**3.32**	2.9
9	KEB	3.15	3.22	3.45	**0.09**	**2.96**	2.8
10	El Bouri	2.99	3.01	3.07	**0.18**	**3.33**	4.6
11	Kazakh	3.6	3.58	3.32	**0.08**	**3.6**	4.5
12	CPC	3.89	3.62	3.89	**0.09**	**2.95**	3.7
13	LSCO	4.24	3.64	3.23	**0.14**	**3.43**	3.9
14	Rhem.	3.86	3.06	3.14	**0.08**	**3.14**	3.4
15	Prinos	4.58	3.72	3.54	**0.15**	**3.35**	3.4
16	Azeri L	4.64	3.82	3.67	**0.06**	**3.69**	4.0
17	SGC	2.96	3.18	3.03	**0.1**	**2.77**	3.1
18	Oryx	3.01	2.54	2.48	**0.1**	**2.75**	3.8
19	Okwuib	6.09	5.34	4.95	**0.12**	**4.95**	5.7
20	RasGharib	2.23	2.35	2.4	**0.59**	**2.75**	3.1
21	Varandey	4.34	3.23	3.46	**0.05**	**3.88**	4.8
22	Arab L	3.58	3.52	3.65	**0.05**	**3.04**	2.5
23	KBT	3.15	3.18	3.34	**0.04**	**2.93**	2.9
24	Tempa Rossa	2.4	2.66	2.75	**0.02**	**2.55**	2.3
25	Forties	3.41	3.11	3.06	**1.25**	**2.89**	4.3
26	Aseng	4.56	3.7	3.59	**0.03**	**4.42**	4.7
27	Kuwait L	3.91	3.89	3.99	**0.06**	**3.14**	3.2
28	Cheleken	5.05	4.49	4.57	**0.08**	**3.97**	3.6
29	Caspian H	3.9	4.75	4.78	**0.03**	**4.17**	4.2
30	Kumkol	3.43	3.55	3.89	**0.97**	**3.53**	4.9
31	Bonga	6.58	5.05	3.73	**0.19**	**4.32**	4.5
32	Forouzan	2.98	2.84	2.77	**0.26**	**2.89**	3.9
33	Bozachi	3.09	2.97	3.59	**0.84**	**3.80**	4.6
34	El Sharara	4.05	3.63	3.59	**0.21**	**3.04**	2.9
35	Helm	3.73	3.72	3.73	**0.03**	**3.38**	2.9

Table 5. TBP fraction yields of Azeri Light crude oil measured in two different laboratories and estimated refinery margins using the refinery LP model (Honeywell Refinery and Petrochemistry modeling System (RPMS)) and employing the TBP distillation yields measured in both laboratories.

Fraction	Az.L. Lab.1, %wt Yield	Az.L. Lab.2, %wt Yield
IBP-182 °C	20.3	22.2
182–355 °C	36.4	31.7
IBP-355 °C	56.7	53.9
355–560 °C	31.2	34.2
IBP-560 °C	87.9	88.1
>560 °C	12.2	11.9
Refinery margin	Base	Base−2 MM USD/month

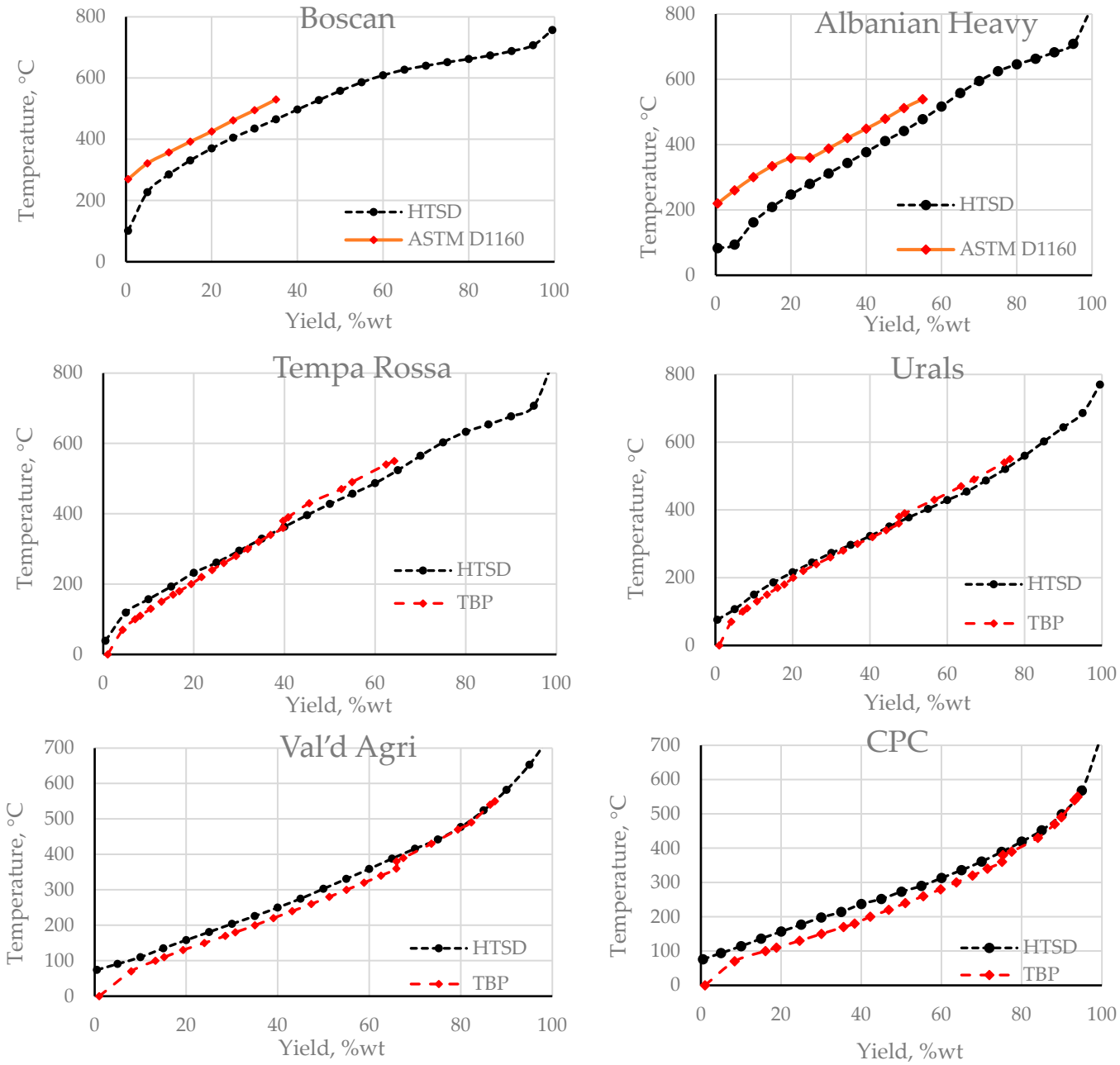

Figure 6. HTSD and TBP distillation curves of heavy-extra heavy (Boscan, Albanian), heavy (Tempa Rossa), medium (Urals), light (Vald'Agri), and extra light (CPC).

The data in Figure 6 exhibits that the high temperature simulated distillation (HTSD, ASTM D7169) reports lower yields for the fractions boiling below 360 °C (the atmospheric part of the TBP—ASTM D 2892) and higher yields for the fractions boiling above 360 °C (the vacuum part of the TBP—ASTM D 5236) for the heavy-extra heavy, heavy, and medium crude oils.

The light, and the extra light crude oils, however, indicate a good coincidence between HTSD and ASTM D 5236, and the typical lower HTSD yields for the fractions boiling below 360 °C. There is still need of additional investigations for development of a reliable method that allows converting the simulated distillation data into TBP data for all crude oil types.

3. Petroleum Characterization by Means of SARA Analysis

Petroleum is a complex mixture of hydrocarbon and non-hydrocarbon components with carbon numbers from 1 to over 100 atoms and boiling points from −161.60 C (methane) to over 760 °C. Using distribution models of TBP of different types of petroleum [5], it has been found that their final boiling temperatures can vary between 1000 and 2000 °C. At a carbon atom number of 25 (boiling point = 402 °C) the number of possible isomers of acyclic alkane isomers amounts to 36.7 × 106, while at a carbon atom number of 100 (boiling point = 708 °C) the number of possible isomers of acyclic alkane isomers amounts to 5920 × 1036 [91]. The actual number of components that go into the composition of a crude oil is unknown, but it is assumed to exceed 10^6 [91,92]. For example, in the heaviest fraction of oil boiling above 540 °C (vacuum residue) only 5% of its constituent components are known, the remaining 95% are unknown to mankind [93]. Analyzing such a complex mixture is a challenge for specialists working in the petroleum, refining and petrochemical industries. Therefore, a separation of the complex petroleum mixture into fractions based on their chemical similarity can facilitate the process of petroleum chemical characterization and petroleum chemistry understanding. The separation of petroleum into saturates, aromatics, resins and asphaltene fractions (SARA) is carried out on the basis of the polarity of these fractions by using different solvents, eluents and adsorbents. The first step in SARA fractionation is the precipitation of the asphaltenes from the oil mixture using n-heptane [92,94] or n-pentane [95]. The de-asphalted petroleum mixture can be further examined for the content of saturates, aromatics, and resinous fractions by ASTM D2007, ASTM D4124, high performance liquid chromatography (HPLC), or thin layer liquid chromatography coupled to a flame ionization detector (TLC-FID; IATROSCAN) methods. Significant differences have been reported between group hydrocarbon composition of oil (SARA) results obtained by ASTM, HPLC or TLC-FID methods [96–98]. The difference in the methods, the nature of the eluent, and the molecular weight of the solvents significantly affect the relative proportions of each fraction [46,95]. SARA results of oil composition have been used by a number of researchers to predict various oil properties, coke formation, stability of asphaltenes in oil, and others [46,99–101]. The group hydrocarbon composition of petroleum is used as input information in a number of equations of state, forming the basis of thermodynamic models predicting sediment formation in the process of petroleum extraction and refining [102–107]. The group hydrocarbon composition of feedstock for conversion to lighter high-value products in a range of conversion processes has been shown to carry valuable information about the operation of these processes [108–117]. Therefore, the investigation of methods for measuring SARA composition of petroleum and petroleum derivatives is of considerable interest for practice. Moreover, different researchers apply different analytical techniques to measure the SARA composition of oil and oil derivatives and often their comparison is impossible. In this review article we summarize a large body of data reported in the literature on the group hydrocarbon composition of extra light, light, medium, heavy, extra heavy oil types, oil sands and natural bitumen obtained from different methods and search for relationships between SARA composition, physicochemical properties of oil and different indices reported in the literature characterizing the oil behavior during the extraction and refining process. In this case, 308 samples of crude oil types of representative of extra light (specific gravity (SG) < 0.8017), light (0.8017 < SG < 0.855), medium (0.8600 < SG < 0.9220), heavy (0.9220 < SG < 1.000), and ultra-heavy (SG > 1.000) were analyzed for SARA composition in 16 literature sources [13,16–30]. Table S5 summarizes the group composition data (SARA), the aromatic structure content (sum of all fractions that contain aromatic carbon. These are aromatic, resinous and asphaltene components) and specific gravity of the 308 petroleum samples. Five methods are mentioned as used for the SARA analysis of crude oil composition and their percentage distribution for the data base of 318 crude oils extracted from the literature sources [118–134] is presented in Table 6.

Table 6. Distribution of employed methods to perform SARA analysis of 308 crude oils.

SARA Analysis Method	% of 318 Crude Oils
ASTM D2007	33.4
Liquid chromatography	15.6
HPLC	37.3
TLC–FID (Iatroscan)	8.8
modified ASTM D4124	4.9

The data in Table 6 shows that the HPLC method has found the most widespread application for SARA petroleum composition analysis. It has been applied to the analysis of the group hydrocarbon composition of all groups of petroleum: extra light, light, medium, heavy, extra heavy petroleum types and oil sands and natural bitumens. The next most common method is the ASTM D2007 method, also applied to all crude oil types. Next, liquid chromatography method follows. It has also found application for the determination of SARA composition of all crude oil groups. The thin layer chromatography TLC-FID (Iatroscan) takes the fourth place of SARA method application. It has found application for SARA analysis of light, medium and heavy crude oil types. The last place method in terms of applicability is the modified ASTM D4124 method. It has also found application for SARA analysis of light, medium and heavy grades of crude oil.

In order to investigate the presence of statistically meaningful relations between the SARA fractions measured by the five methods used for oil group hydrocarbon composition analysis, intercriteria analysis (ICrA) evaluation for all methods was performed. The results of ICrA evaluations are summarized in Tables S6–S15. The ICrA approach has been applied in several our studies to search for statistically meaningful relations in petroleum characterization and refining [9]. More detailed explanation of the essence of ICrA and its application in petroleum refining the reader can find in our recent study [54]. Here, we summarize the meaning of the values of positive and negative consonance (μ) and (υ) applied in ICrA evaluation of the studied petroleum property relations. The meaning of $\mu = 0.75 \div 1.00$; $\upsilon = 0 \div 0.25$ denotes a statistically meaningful significant positive relation, where the strong positive consonance exhibits values of $\mu = 0.95 \div 1.00$; $\upsilon = 0 \div 0.05$, and the weak positive consonance exhibits values of $\mu = 0.75 \div 0.85$; $\upsilon = 0.25 \div 0.15$. Respectively, the values of negative consonance with $\mu = 0.00 \div 0.25$; $\upsilon = 0.75 \div 1.00$ means a statistically meaningful negative relation, where the strong negative consonance exhibits values of $\mu = 0.00 \div 0.05$; $\upsilon = 0.95 \div 1.00$, and the weak negative consonance exhibits values of $\mu = 0.15 \div 0.25$; $\upsilon = 0.75 \div 0.85$. From the data presented in Tables S6–S15, it can be seen that all the methods for SARA analysis of crude oil except thin layer chromatography (correlation analysis) show statistically significant relationship between saturate components and aromatic structure contents with the specific gravity of crude oil. The ASTM D 2007, ASTM D 4124 and high-performance liquid chromatography methods show a moderate statistically significant relationship between the saturate components and aromatic structure content and the specific gravity of the crude oil, and the liquid chromatography method demonstrates a strong statistically significant relationship between these crude oil parameters. A similar relationship between specific gravity and the content of saturate components and aromatic structures was found in our recent study for vacuum residues derived from all groups of oil types [135]. From this it can be concluded that the specific gravity of crude oil and petroleum derivatives is a major indicator characterizing the chemical nature of oil. By using the nonlinear least squares method, a mathematical relationship was derived relating the specific gravity of crude oil to the content of aromatic structures. This relationship is shown by Equation (7) and in Figure 7.

$$\text{ARO str.} = \frac{100}{0.2748 + 5.198e^{-4.787SG}} - 239 \quad (7)$$

where, ARO str. = Aromatic structures content, %wt; SG = specific gravity.

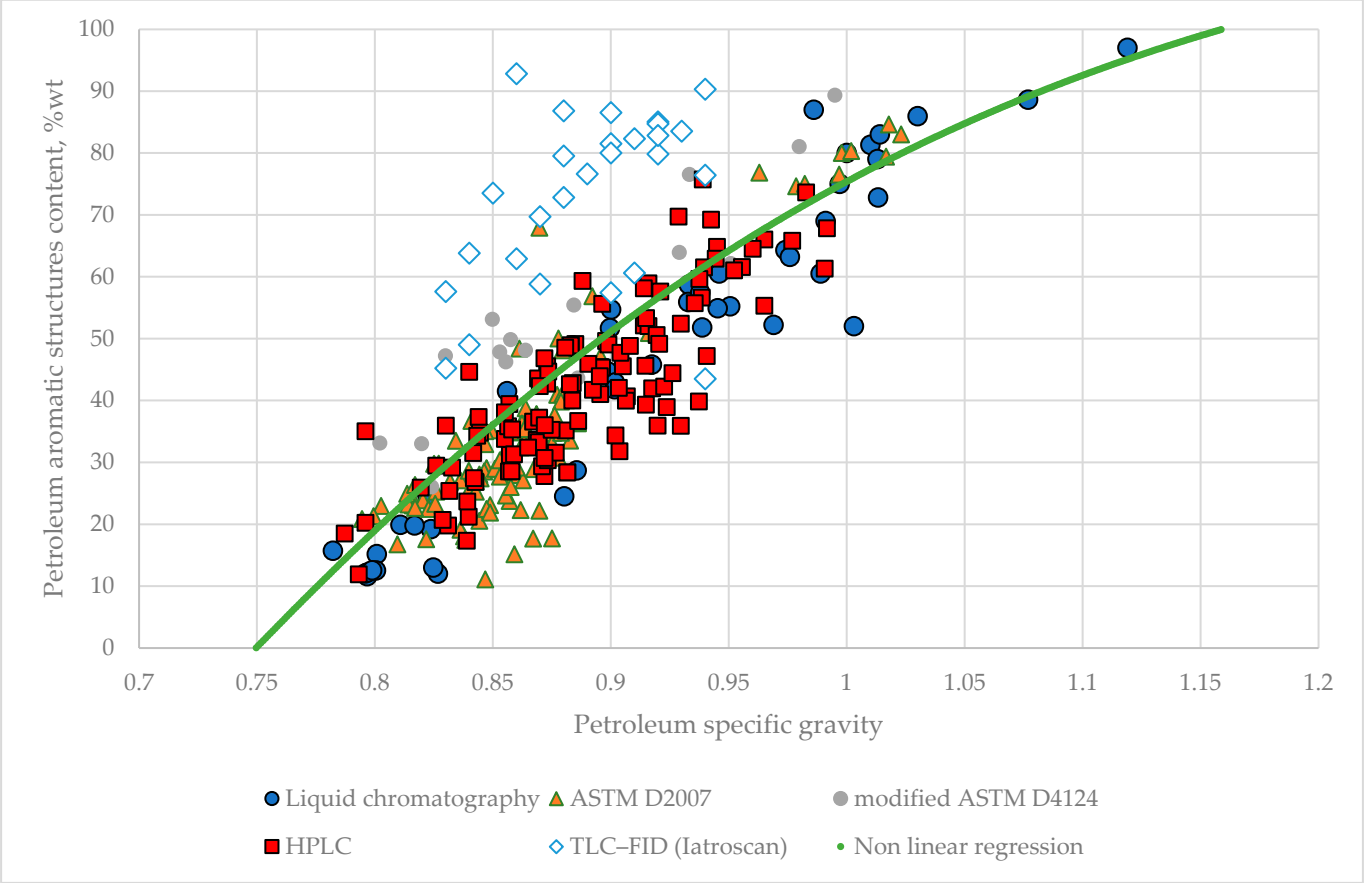

Figure 7. Dependence of petroleum aromatic structures content on specific gravity.

The average absolute deviation of the values predicted by equation 7 for the aromatic structure content of the crude oils from those of the measured values, excluding the data from the Iatroscan analysis, is 7.5%. Our previous studies [135] have shown that when the deviation of the predicted from the measured values of the aromatic structure content is greater than the mean absolute deviation this suggests an incorrect analysis and it should be repeated. Not obeying this dependence for SARA analysis data performed by the thin layer chromatography (TLC, Iatroscan) method indicates disagreement of this analysis method with the other methods, a fact already commented in other studies expressing distrust in the results of this analysis due to the large errors made when the same sample is analyzed repeatedly [26]. The reason for the inaccurate SARA analysis by thin layer chromatography (TLC, Iatroscan) has been attributed to the problem of highly adsorbed asphaltenes not migrating along the chromatographic rod [136].

Our analysis of SARA composition data of extra light, light, medium, heavy, extra-heavy crude oil types, oil sands and natural bitumen published in the literature, as well as our own investigations with different methods to determine the SARA composition of vacuum residues of different crude oil types confirm the significant deviation of the SARA fraction relationships observed between the four SARA analysis methods (ASTM D 2007, ASTM D 4124, HPLC, and liquid chromatography (LC)) and the Iatroscan method [26]. From this it can be concluded that the results of thin layer chromatography are incomparable to the other analysis methods and that this analysis method has a high uncertainty according to the studies of Youtcheff [136]. It can be seen from the data in Tables S6–S15 that the relative proportion of resin-asphaltene components increases with increasing aromatic content and crude oil density. In other words, the increase in specific gravity is associated not only with an increase in aromatic structures content in the crude oil, but also with an increase in the relative proportion of resin-asphaltenic components at the expense of

a decrease in the relative proportion of aromatic components. It can also be noted that an increase in the content of saturate components is statistically significantly correlated with an increase in the value of the index of colloidal instability, suggesting that crude oil types that have a higher content of saturate components may be colloidally unstable and contribute to an increase in the rate of sedimentation during production and processing. This fact is also confirmed in the studies of Xiong et al. [129], reporting that sedimentation problems in the oil recovery process occur significantly more frequently in light types than in other oil types. Unfortunately, the crude oil SARA method applied to lighter crude oils is associated with a mass balance inaccuracy as reported by Hemmingsen [134] and illustrated in Table 7

Table 7. Variation of SARA fractions yields obtained during the use of HPLC method with crude oil density at 20 °C [134].

Crude Oil Density at 20 °C, g/cm^3	SARA Fractions Total Yield, %wt
D20 < 0.86	≈73%
0.87 > D20 > 0.86	≈82%
0.88 > D20 > 0.87	≈90%
0.89 > D20 > 0.88	≈83%
0.90 > D20 > 0.89	≈89%
0.96 > D20 > 0.92	≈96%
D20 > 0.96	≈100%

Note: D20 = crude oil density at 20 °C, g/cm^3.

This shortcoming could be overcome by the use of prediction methods as that reported by Yarranton [137]. He reported a higher accuracy of SARA composition prediction based on crude oil high temperature simulated distillation, and asphaltene content, than the typical crude oil SARA analysis. This may be well applied to lighter crude oils where the losses, as evident from the data in Table 7, are quite high. The SARA analysis of a crude oil could be reconstituted by the use of developed correlations to predict the content of aromatic structures, or saturates, which is the difference 100—content of aromatic structures, in the crude oil fractions having information for fraction boiling point and density (specific gravity). Such correlations are summarized below.

The calculation of the saturate content of the vacuum residue fraction (>550 °C) can be performed following the model developed in [135]. It is given as Equation (8).

$$\text{VR saturate} = 100 - \frac{100}{0.16137823 + 1000e^{-11.732948}d_{VR}} - 516 \quad (8)$$

The calculation of the saturate content of the vacuum gas oil fraction (360–550 °C) can be carried out following the model developed in [138]. It is given as Equation (9).

$$\text{VGO Saturates} = -1.867 + 0.9103\left(100 - \frac{100}{0.4426 + 547.9e^{-8.719}d_{VGO}} - 113.1\right) + 9.3398\text{ARI}^{-2} \quad (9)$$

The aromatic ring index (ARI) is calculated by the correlation of Abutaqiya et al. [139,140] as shown in Equation (10).

$$\text{ARI} = f(\text{MW}, F_{RI}) = \frac{2[\frac{\text{MW}}{F_{RI}} - (3.5149\text{MW} + 73.1858)]}{(3.5074\text{MW} - 91.972 - (3.5149\text{MW} + 73.1858))} \quad (10)$$

The molecular weight of oil fractions can be calculated by the correlation of Goosens [49] as shown in Equation (11)

$$\text{MW} = 0.010770T_b^{[1.52869 + 0.06486\ln(\frac{T_b}{1078 - T_b})]}/d \quad (11)$$

The refractive index of oil fractions can be estimated by the correlation of Stratiev et al. [141] as shown in Equation (12):

$$RI_{LNB} = 0.702091d_{15} - 0.00011T_{50} + 0.91493 \quad (12)$$

The function of refractive index can be estimated by Equation (13) [139,140].

$$F_{RI} = \frac{n_{D20}^2 - 1}{n_{D20}^2 + 2} \quad (13)$$

The saturate content in diesel fraction (240–360 °C) can be calculated based on the correlation developed in our earlier study [142] and shown as Equation (14):

$$\text{Diesel Saturate} = 100 - \frac{71.37 - \text{Cetane index}}{0.6371} \quad (14)$$

The saturate content in kerosene fraction (180–240 °C) can be calculated based on the correlation developed in our earlier study [142] and shown as Equation (15).

$$\text{Kerosene Saturate} = 100 - \frac{56.605 - \text{Cetane index}}{0.4907} \quad (15)$$

Unfortunately, the saturate content of naphtha fraction (IBP-180 °C) does not correlate with density, and boiling point in contrast to the other crude oil fractions. Investigating the relation of properties of naphtha fractions derived from 244 different crude oils it was found that the content aromatics, or 100—aromatics = saturates does not correlate with any studied property as shown in the data of Tables 8 and 9.

Table 8. μ-values of the Intercriteria analysis evaluation of relations between properties of naphtha fractions derived from 244 different crude oils.

Mu	SG	VABP	Kw	Sulphur	Naphthenes	Aromatics	RON
SG	1.00	0.46	0.02	0.46	0.71	0.66	0.86
VABP	0.46	1.00	0.51	0.52	0.53	0.40	0.46
Kw	0.02	0.51	1.00	0.54	0.28	0.32	0.13
Sulphur	0.46	0.52	0.54	1.00	0.49	0.48	0.48
Naphthenes	0.71	0.53	0.28	0.49	1.00	0.43	0.74
Aromatics	0.66	0.40	0.32	0.48	0.43	1.00	0.62
RON	0.86	0.46	0.13	0.48	0.74	0.62	1.00

Note: Green colour means statistically meaningful positive relation; Red colour implies statistically meaningful negative relation. The intensity of the colour designates the strength of the relation. The higher the colour intensity, the higher the strength of the relation is. Yellow colour denotes dissonance.

Table 9. υ-values of the Intercriteria analysis evaluation of relations between properties of naphtha fractions derived from 244 different crude oils.

Nu	SG	VABP	Kw	Sulphur	Naphthenes	Aromatics	RON
SG	0.00	0.50	0.97	0.54	0.28	0.33	0.13
VABP	0.50	0.00	0.44	0.44	0.44	0.56	0.50
Kw	0.97	0.44	0.00	0.45	0.70	0.66	0.86
Sulphur	0.54	0.44	0.45	0.00	0.50	0.51	0.51
Naphthenes	0.28	0.44	0.70	0.50	0.00	0.57	0.26
Aromatics	0.33	0.56	0.66	0.51	0.57	0.00	0.37
RON	0.13	0.50	0.86	0.51	0.26	0.37	0.00

Note: Green colour means statistically meaningful positive relation; Red colour implies statistically meaningful negative relation. The intensity of the colour designates the strength of the relation. The higher the colour intensity, the higher the strength of the relation is. Yellow colour denotes dissonance.

This is very well illustrated with the data shown in a correlation matrix of naphtha fraction properties of 244 crude oil.

The data in Tables 8 and 9 indicates that only research octane number (RON) of naphtha statistically meaningful correlates with the specific gravity. Therefore, to reconstruct the crude oil SARA composition from data of density and boiling point of the crude oil fractions, requires also information about the saturate content (100-aromatics) in the naphtha fraction, that can be obtained by GC PIANO analysis. By following such a reconstitution method, and employing GC PIANO analysis of naphtha fraction can be avoided the errors in crude oil SARA composition in cases where the SARA mass balance is poor.

4. Advanced Techniques in Petroleum Characterization

Detailed molecular characterization of crude oil remains a challenge for analytical chemists because of its inherently complex nature expressed by enormous number compounds larger than the number of genes in the human genome [143,144]. The accessible detailed molecular-level compositional information of petroleum can be obtained by the sophisticated techniques as mass spectrometry, comprehensive gas chromatography, and hybrid analytical platforms [10,145–150]. A significant amount of research has been given and announced on the characterization of crude oil, coal liquefaction products, and bitumens [151–161] and a huge number of high boiling crude oil molecules were mass resolved and formula identified. Marshall et al. have postulated a special term "Petroleomics" for this field of research [143,162,163].

Mass spectrometry has played a critical role in the characterization of petroleum. High field Fourier transform ion cyclotron resonance (FT-ICR) mass spectrometers are now common in petroleum R&D centers [10]. The usage of a 21 Tesla Fourier transform ion cyclotron resonance mass spectrometer (21 T FT-ICR MS) has shown to be capable of producing unmatched breadth and depth of compositional information lately [145]. Moreover, the combination of mass spectrometry and chromatography, including gas chromatography (GC), 2D GC (GC×GC), high-performance liquid chromatography (HPLC), and gel permeation chromatography (GPC), has enabled a greater understanding on the types and amounts of certain chemical classes in crude oil. Other general techniques employed for organic compounds such as NMR (nuclear magnetic resonance), IR (infrared spectroscopy), Raman, Terahertz, UV–Vis (ultraviolet–visible spectroscopy), and X-ray diffraction clash with the broad range of compounds found in petroleum, generating inapprehensibly complex data [146,164]. Figure 8 summarizes the spectroscopic methods for petroleum properties characterization presented by Correa Pabon and Souza Filho in [164]. Separating petroleum into different fractions prior to crude oil analysis has been demonstrated to be critically important [144,146,162].

Petroleum fractionation helps to improve the dynamic range of the mass spectrometry analysis, molecular structural assignments and simplifies species quantitation by assuming uniform ionization of chemical species with similar structures in the same fraction that have similar ionization efficiency [162]. Certainly, petroleum assay without fractionation is desirable because it is faster and cheaper, but only electron ionization can ionize all crude oil compound classes [165]. In addition, the electron ionization causes extensive fragmentation to many of the compounds in crude oil. All other ionization methods apply to specific classes of compounds.

Different separation approaches have been developed by analytical laboratories with aim to achieve more detailed fractionation of petroleum [158,166–181]. Main separation techniques are chromatography, fractionation (distillation), and solubility-based separations. The commonly used approach for petroleum fractionation into distinct chemical/solubility types is a separation based on saturates, aromatics, resin, and asphaltenes by high-performance liquid chromatography [165,166]. Bissada et al. applied an automated multi-dimensional high-performance liquid chromatography [166,167]. Another separation approach for petroleum separation was proposed by Robson et al. [168] applying a petroleum separation in strong cation-exchange (SCX) solid phase extraction (SPE) car-

tridge. Robbins et al. proposed a separation method based on ion exchange and normal phase chromatography (HPLC-2) [169]. The newest improvement in high-performance liquid chromatography petroleum separation is developed by Putman et al. [170] and includes a dual-column aromatic ring class separation (HPLC-3). The separation of saturated and aromatic hydrocarbons as well as aromatic/aliphatic sulfides is improved and optimized to 1-, 2-, 3-, 4-, and 5+-ring constituents.

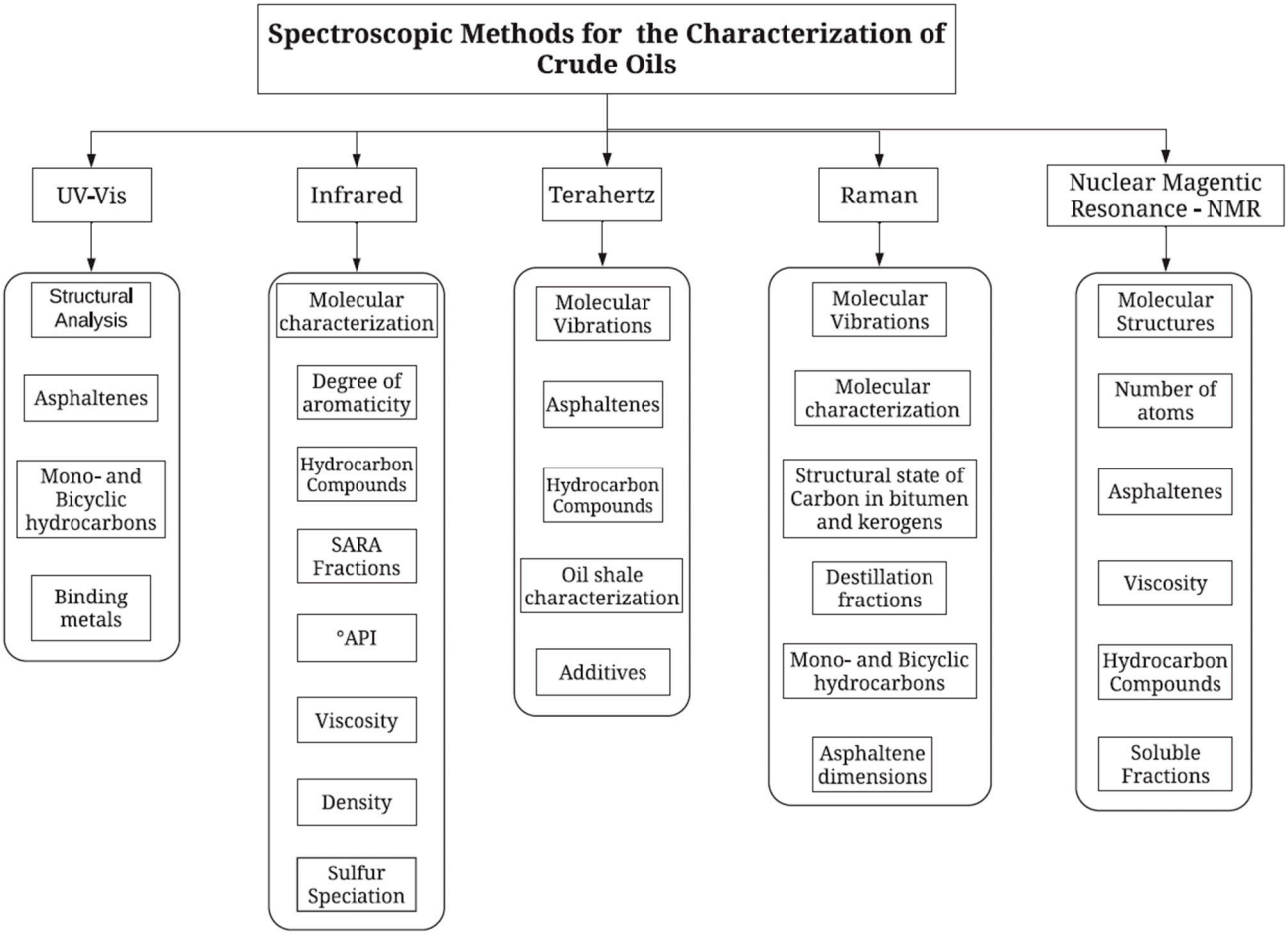

Figure 8. Spectroscopic methods for petroleum properties assay. (Adapted with permission from Ref. [164] Copyright 2019, copyright Elsevier).

A new approach called distillation precipitation fractionation mass spectrometry (DPF MS) for molecular profiling of crude oil and condensates was developed by Yerabolu et al. [174] and Alzarieni et al. [176]. This method is based on segregating petroleum into six distinct fractions containing different types of components (involved initial distillation of vaporous components followed by precipitation of asphaltenes) and then optimizing the ionization method and mass spectrometry technique for the analysis of each fraction. DPF MS method gave weight percentage of each fraction and accurate average molecular weight of the crude oil was derived by combining the average molecular weight and the mass of each fraction [144,174,176].

Selective separation of hetero-organic hydrocarbons from petroleum as naphthenic acids, nickel and vanadyl petroprophrins, nitrogen and sulfur compounds is another field that deserves research attention. Generally, two methods for naphthenic acid separation from crude oil are reported in the open literature: liquid-liquid extraction [182–187] and solid-phase extraction [188–202]. Irrespective of its operationally and relatively low cost, the employment of this process includes a large volume of solvents, and its efficiency can be detracted in samples with low analyte concentration because of amenability to form stable emulsions [192]. More selective methodologies, that minimize solvents, have been

reported [192,193]. Method for tetraprotic acids isolation from petroleum by the use of molecularly imprinted polymers demonstrated a detection of very low concentrations (subparts per million) [193].

Selective isolations of various sulfur types, such as sulfides, thiophenes, and mercaptans is presented in several research [194–196]. Although quite powerful techniques have resulted and are available today for routine use as oxidation, methylation, reduction and liquid-liquid extraction, it is still not possible to obtain clean class separations of all sulfur functional groups [49]. For example, disulfides separation remains an unsolved problem, and no reliable separation principle exists for their analysis in fossil materials [194].

Metal petroprophrins isolation is another active area of research [199–201]. Qian et al. developed a cyclograph separation scheme for nickel porphyrins fractionation [200]. In addition, a combination of solvent extraction, silica gel, and aluminum column separations is proposed in [201] that allowed isolation of ultrahigh purity vanadyl petroprophrins.

Ultrahigh resolution and accuracy mass spectrometry is a wide used tool to characterize crude oils and its derivatives [144,146,202–207]. FT-MS can be performed in ion cyclotron resonance (ICR) [144,146,204,206–212], orbitrap mass spectrometers [202,213–215], and additional non-Fourier transform techniques, such as high-resolution time-of-flight mass spectrometry (TOF-MS) [216,217]. FT-ICR MS is the state-of-the-art for determination of elemental compositions of compounds in complex mixtures as petroleum due to its ultrahigh resolving power and accuracy. The basic principles of FT-ICR MS instrumentation, ionization techniques and data interpretation were reviewed in [144,146,218]. Electrospray ionization (ESI) is the most common ionization technique that has been used which is suitable for the gentle ionization of the polar (acidic and basic) components. Negative ESI (−) selectively ionizes acids, phenols, and non-basic nitrogen compounds, while positive ESI(+) selectively ionizes basic nitrogen compounds. ESI(−) FT-MS has been applied in different cases, such as to characterize polar heteroatomic components before and after hydro-treatments, naphthenic acids, and heavy oil distillation cuts [183,185,219–221]. In addition, ESI (−) 7.2 T FT-ICR MS has been employed to evaluate the crude oil biodegradation level by profiling the changes in relative abundances of compounds in the heteroatom classes, in particular, oxygen containing compounds [212,213]. Guricza et al. applied ESI (−) FT-MS for measurement of non-polar polyaromatic hydrocarbons and polyaromatic heterocycles in heavy crude oil asphaltenes [222]. Other ionization methods that have been found to provide complementary information on the less polar or more volatile constituents of petroleum are atmospheric pressure techniques. For example, atmospheric pressure photoionization (APPI), atmospheric pressure chemical ionization (APCI), atmospheric pressure laser ionization (APLI) and laser desorption ionization (LDI) has been used to better characterize the aromatic hydrocarbons and asphaltenes in crude oil [154,205,223–226]. APPI outperforms other ionization methods (such as APCI) as it generates mostly odd-electron molecule ions for aromatic molecules without fragmentation.

FT-ICR MS and Orbitrap-MS were compared as tools for the study of nonvolatile crude oil fraction composition by Vanini et al. [227]. Both techniques enabled the elemental composition to be derived by precise mass measurements, and the most plentiful components were mainly N, N2, O3, O1, O2, NO2, NS, NOS, and OS classes. FT-ICR MS facilitated the finding of higher molecular weight analytes in relation to Orbitrap-MS [227].

Ionization of large, saturated hydrocarbon is the greatest challenge in petroleum assay by MS techniques. These petroleum constituents are not volatile and do not contain easily ionizable functional groups. ESI, matrix-assisted laser desorption/ionization (MALDI), field desorption, field ionization and APCI have been reported in the literature for ionization of large, saturated hydrocarbons [228–230], but one should always critically evaluate and, if possible, tailor the ionization conditions to be most suitable for the petroleum sample being analyzed [144].

Significant advances in the chemical characterization of petroleum has been achieved by applying of two-dimensional gas chromatography (GC×GC). Implementing of a polar column followed by a nonpolar column improves the separation of saturated and aromatic

hydrocarbons in petroleum distillates [231,232]. Combination of two-dimensional gas chromatography with (+) EI TOF MS give opportunity to determine separating compounds in an oxidized heavy saturated hydrocarbon fraction [233], naphthenic acids separated from petroleum [234], composition of a heavy crude oil and to generate a template that can be used to simulate its distillation [235]. In addition, separation of some isomers of large saturated hydrocarbons and their sulfides from Venezuelan crude oil sample by applying of GC×GC/(+) EI TOF MS have been reported [236].

Vanini et al. [237] offered a method to analyze vaporous hydrocarbons by GC×GC/(+) EI TOF MS and (−) ESI 9.4 T FT-ICR MS to analyze acidic compounds in the same crude oil samples. Various groups of components were identified by using GC×GC/(+) EI TOF MS, including linear, branched, and cyclic saturated hydrocarbons, alkylbenzenes, alkylnaphthalenes, alkylindanes, pyrenes, and fluorenes in petroleum samples with different density [144,237].

Integration of three analytical techniques, high-performance liquid chromatography (HPLC) ring-type separation, two-dimensional nuclear magnetic resonance spectroscopy (2D NMR), and ultrahigh-resolution mass spectrometry (MS), for molecular-level characterization of crude oil was employed by Kim et al. [238] for detailed characterization of its compositions (Figure 9).

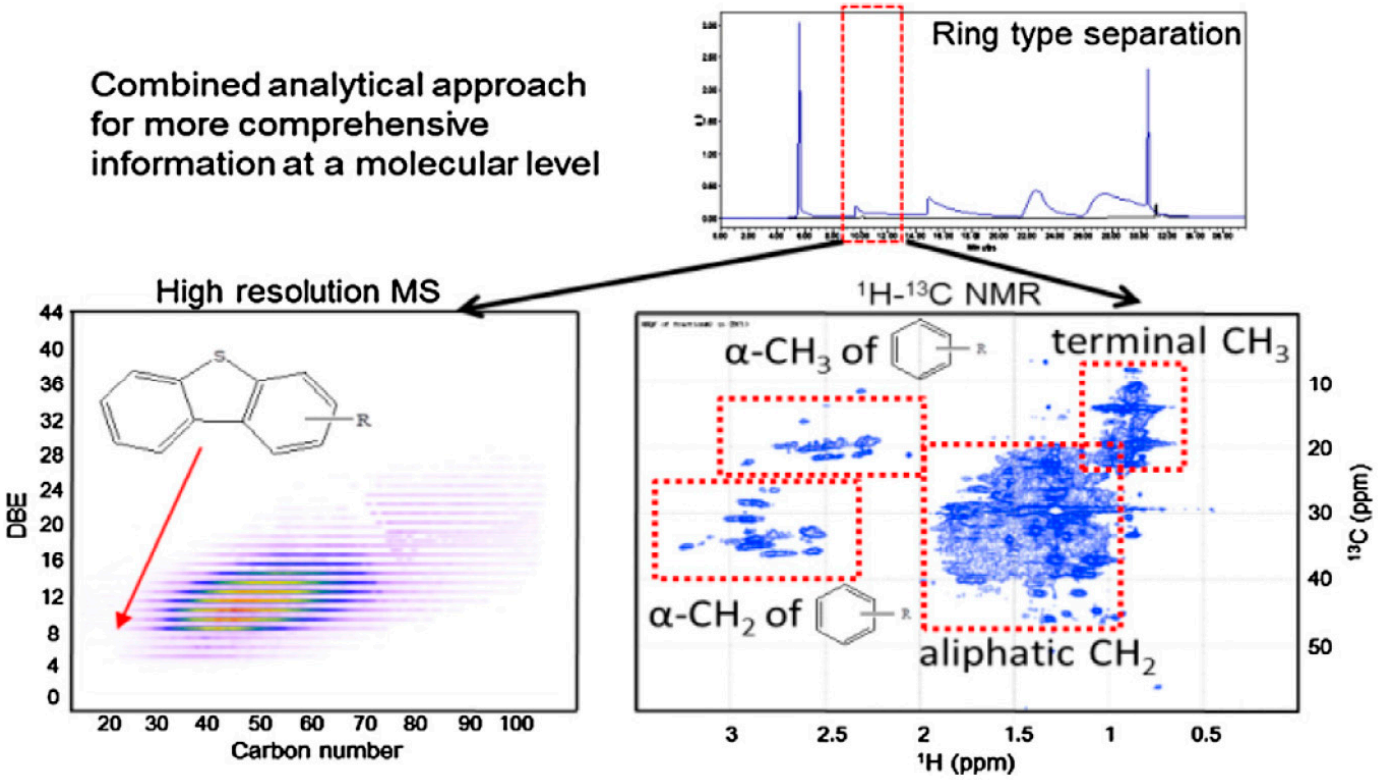

Figure 9. Combined analytical approach proposed by Kim et al. [238]. (Adapted with permission from Ref. [238] Copyright 2017, copyright Elsevier).

HPLC ring type separation was used to obtain five petroleum fractions. The features of each fraction obtained by three techniques complied well and the aromaticity enhanced as the fraction number magnified. Additionally, 2D NMR data and double bond equivalence (DBE) distribution derived from high-resolution-MS, it was shown that the first to third fractions of HPLC ring type separation contained hydrocrabon group components with an aromatic ring core and multiple saturated cyclic rings. The structures and distribution of heteroatom group components could be clarified based on combined information on the HPLC elution order and the class and DBE distributions seen using ultrahigh-resolution mass spectrometry [238].

Nuclear magnetic resonance (NMR) and infrared (IR) spectroscopy are two analytical methods that generate a large volume of compositional information [12]. Many studies have appeared recently which suggest approaches based on application of 1H and 13C NMR and near (NIR) and mid (MIR) infrared spectroscopy techniques associate with chemometrics to predict crude oil properties [12,120,239–250]. Data obtained by1H and 13C NMR and near (NIR) and mid (MIR) infrared spectroscopy techniques are used as an input data for modeling petroleum properties by applying of the regression techniques as principal component regression (PCR) [242], multiple linear regression (MLR) [250], partial least square PLS [242,247,248] and artificial neural network (ANN, random forest) [241]. Many of the recently published studies continued to apply linear PLS [239,245,251,252] for petroleum properties modeling on the base of NIR and MIR spectra because of its simplicity and effectiveness for data with linear behavior. Most of petroleum bulk properties can be defined directly. For some properties such as density, and TBP curve, the relation between spectrum and property is implicit due to the absence of absorption band defined by these properties [12]. Actually, the spectra are related to some other component, which in turn is proportional to the modeled property. To the best of our knowledge, no reports have appeared yet to predict petroleum salt and ash content based on NIR and MIR spectra.

5. Conclusions

Petroleum is a complex mixture of hydrocarbon and non-hydrocarbon components with carbon numbers from 1 to over 100 atoms and boiling points from −161.60 C (methane) to over 760 °C. Detailed molecular characterization of crude oil remains a challenge for analytical chemists because of its inherently complex nature expressed by enormous number compounds larger than the number of genes in the human genome. Crude oil is not a homogeneous raw material. Each crude oil produced in the world has a unique chemical composition, which varies according to the manner of its formation. Thus, no two crude oils are the same. That is why the petroleum characterization remains a challenge for both crude oil producers and petroleum refiners. The literature search indicates that the petroleum characterization can be classified in three categories: crude oil assay; SARA characterization; and molecular characterization (advanced techniques in petroleum characterization). The crude oil assays are comprehensive and short (inspection) and their heart is the true boiling point distillation analysis. The employment of probability distribution functions to fit TBP distillation data allows constructing of a correct TBP curve and may detect measurement errors. The six parameter Weibull extreme function showed to best fit the TBP data of all crude oil types. Although the GC simulated distillation is the best candidate for substitution of the costly and time consuming TBP analysis additional investigations are required to develop a reliable correlation applicable to all petroleum crude types.

To the best of our knowledge for the first time the application of the additive rule to predict crude oil asphaltene content from that of the vacuum residue multiplied by the vacuum residue TBP yield was examined in this work. It was found that the measured petroleum asphaltene content is in general higher than that of the estimated one using the additive rule. It was also discovered that a strong linear relation between the contents of C_5- and C_7-asphaltenes in crude oil and derived thereof vacuum residue fraction exists. It was found that a strong linear relation between the contents of C_5- and C_7-asphaltenes in crude oil and derived thereof vacuum residue fraction exists. This allows at presence of available information for the content of C_7-asphaltenes to compute the content of C_5-asphaltenes. The difference between C_5- and C_7-asphaltenes defines the C_5-resins and in case of available information about saturate content in the crude oil the full SARA composition can be obtained. A significant amount of literature has been analyzed for the SARA composition of extra light, light, medium, heavy and extra heavy crude oil types, oil sands and bitumens. It was found that the most used method for SARA analysis of petroleum is HPLC and ASTM D 2007, followed by liquid chromatography method. The thin-layer chromatography (TLC, Iatroscan) method reported results significantly different from those of the other methods, and it is reported to have a higher uncertainty. An equation was derived that

predicts the aromatic structure content of crude oil from its density with an average absolute deviation of 7.5%. An increase in crude oil density is associated not only with an increase in the content of aromatic structures, but also with an increase in the relative proportion of resin-asphaltene components in these aromatic structures. Crude oil types with higher content of saturate components have higher colloidal instability index, which implies a greater propensity to sediment formation in the process of their extraction and processing. A new SARA reconstitution approach is proposed to overcome the poor SARA analysis mass balance when crude oils with lower density are analyzed.

The rapid development of analytical technique and application of combination of various advanced techniques has made possible to identify a large fraction of petroleum molecules. Unfortunately, there are still problems with the identification of the heavy part of the crude oil, such as heavy saturated hydrocarbons ionization, complex asphaltene molecules, and some heteroatom compounds. Finally, the employment of a chemometric method integrated with spectroscopic data is very helpful in extracting information about the composition of complex crude oil matrices consisting of a great number of compounds.

Supplementary Materials: The following supporting information can be downloaded at: https://www.mdpi.com/article/10.3390/en15207765/s1, Table S1: Comprehensive assay of extra light, light, medium, heavy, and heavy-extra heavy crude oils from all over the world; Table S2: TBP characterization (ASTM D-2892; up to 360 °C, and ASTM D-5236; >360 °C) of extra light, light, medium, and heavy crude oils; Table S3: Density at 15 °C of TBP crude fractions of extra light, light, medium, and heavy crude oils; Table S4: Sulphur content of TBP crude fractions of extra light, light, medium, and heavy crude oils; Table S5: SARA (Saturates, Aromatics, resins, asphaltenes) of 308 samples of extra light, light, medium, heavy, and extra heavy crude oils; Table S6: μ-values of the Intercriteria analysis evaluation of relations between SARA fractions and specific gravity of the studied crude oils by the ASTM D 2007 method (103 crude oil samples); Table S7: υ-values of the Intercriteria analysis evaluation of relations between SARA fractions and specific gravity of the studied crude oils by the ASTM D 2007 method (103 crude oil samples); Table S8: μ-values of the Intercriteria analysis evaluation of relations between SARA fractions and specific gravity of the studied crude oils by the HPLC method (116 crude oil samples); Table S9: υ-values of the Intercriteria analysis evaluation of relations between SARA fractions and specific gravity of the studied crude oils by the HPLC method (116 crude oil samples); Table S10: μ-values of the Intercriteria analysis evaluation of relations between SARA fractions and specific gravity of the studied crude oils by the liquid chromatography method (47 crude oil samples); Table S11: υ-values of the Intercriteria analysis evaluation of relations between SARA fractions and specific gravity of the studied crude oils by the liquid chromatography method (47 crude oil samples); Table S12: μ-values of the Intercriteria analysis evaluation of relations between SARA fractions and specific gravity of the studied crude oils by the modified ASTM D 4124 method (15 crude oil samples); Table S13: υ-values of the Intercriteria analysis evaluation of relations between SARA fractions and specific gravity of the studied crude oils by the modified ASTM D 4124 method (15 crude oil samples); Table S14: Correlation matrix of SARA fractions and specific gravity of the studied crude oils by the TLC method (27 crude oil samples).

Author Contributions: Conceptualization, D.S. and I.S.; methodology, D.S. and I.S.; software, S.N. and S.R.; validation, I.V.K.; formal analysis, S.N.; investigation, V.I.; resources, K.A.; data curation, S.R.; writing—original draft preparation, D.S. and I.S.; writing—review and editing, D.S. and I.S.; visualization, D.N.; supervision, K.A.; project administration, K.A.; funding acquisition, K.A. All authors have read and agreed to the published version of the manuscript.

Funding: This research received no external funding.

Data Availability Statement: Not applicable.

Acknowledgments: The authors Krassimir Atanassov, and Simeon Ribagin acknowledge the support from the Bulgarian National Science Fund under Grant Ref. No. KP-06-N22-1/2018 "Theoretical research and applications of InterCriteria Analysis".

Conflicts of Interest: The authors declare no conflict of interest.

Nomenclature

AAD	Absolute average deviation
a_1, a_2, a_3, a_4, a_5, a_6	Parameters statistically fitted to experimental data
A, B	Boiling point distribution model parameters
ANN	Artificial neural network
API	API gravity
APCI	Atmospheric pressure chemical ionization
APLI	Atmospheric pressure laser ionization
APPI	Atmospheric pressure photoionization
ARI	Aromatic ring index
ARO str.	Aromatic structures content
Asph	Asphalthenes
AR	Atmospheric residue
CCR	Conradson carbon residue
DPF MS	Distillation precipitation fractionation mass spectrometry
d_{vgo}	Vacuum gas oil density at 15 °C
GC	Gas chromatography
GPC	Gel permeation chromatography
ESI	Electrospray ionization
FID	Flame ionization detector
FT-ICR	Fourier-transform ion cyclotron resonance
F_{RI}	Function of refractive index
H/C	Hydrogen to carbon ratio
HPLC	High performance liquid chromatography
HTSD	High temperature simulated distillation
IR	Infrared spectroscopy
K_w	Watson characterization factor
LC	Liquid chromatography
LDI	Laser desorption ionization
LP	Linear programing
MIR	Mid infrared spectroscopy
MON	Motor octane number
MLR	Multiple linear regression
MS	Mass spectrometry
MW	Molecular weight
N	Nitrogen
NIR	Near infrared spectroscopy
NMR	Nuclear magnetic resonance spectroscopy
OCs	Opportunity crude oils
PCR	Principal component regression
PIANO	Paraffins, iso-paraffins, aromatics, naphthenes, olefins
PLS	Partial least square
RI or n_{D20}	Refractive index at 20 °C
RON	Research octane number
RPMS	Refinery and petro-chemistry modeling system
S	Sulfur
SARA	Saturates, aromatics, resins, asphalthenes
SCX	Strong cation exchange
SG	Specific gravity
SPE	Solid phase exchange
T_{50}	Average boiling point
T_i	Absolute boiling point, K

T_o	Boiling point at xi = 0, K
TAN	Total acid number
TBP	True boiling point
TOF-MS	time-of-flight mass spectrometry
TLC	Thin layer chromatography
2D NMR	Two-dimensional nuclear magnetic resonance spectroscopy
UV-VIS	Ultraviolet–visible spectroscopy
VABP	Volume average boiling point
VGO	Vacuum gas oil
VIS	Viscosity
VR	Vacuum residue
x_i	Cumulative weight fraction

References

1. Speight, J.G. *The Chemistry and Technology of Petroleum*, 5th ed.; CRC Press: Boca Raton, FL, USA, 2014. [CrossRef]
2. Ramirez-Corredores, M. *The Science and Technology of Unconventional Oils*; Elsevier: Cambridge, MA, USA, 2017; Available online: https://www.elsevier.com/books/the-science-and-technology-of-unconventional-oils/ramirez-corredores/978-0-12-801225-3 (accessed on 16 September 2022).
3. Altgelt, K.; Boduszynski, M. *Composition and Analysis of Heavy Petroleum Fractions*, 1st ed.; CRC Press: Boca Raton, FL, USA, 2014. [CrossRef]
4. Ovalles, C.; Moir, M.E. *The Boduszynski Continuum:Contributions to the Understanding of the Molecular Composition of Petroleum*; ACS Symposium Series; ACS: Washington, DC, USA, 2018; p. 1282.
5. Stratiev, D.S.; Dinkov, R.K.; Shishkova, I.K.; Nedelchev, A.; Tsaneva, T.; Nikolaychuk, E.; Sharafutdinov, I.; Rudnev, N.; Nenov, S.; Mitkova, M.; et al. Investigation on feasibility to simulate distribution of boiling point and molecular weight of heavy oils. *Pet. Sci. Technol.* **2015**, *33*, 527–541. [CrossRef]
6. Riazi, M.R. A Continuous Model for C_{7+} Fraction Characterization of Petroleum Fluids. *Ind. Eng. Chem. Res.* **1997**, *36*, 4299–4307. [CrossRef]
7. Riazi, M.; Al-Adwani, H.; Bishara, A. The impact of characterization methods on properties of reservoir fluids and crude oils: Options and restrictions. *J. Pet. Sci. Eng.* **2004**, *42*, 195–207. [CrossRef]
8. Mitkova, M.; Stratiev, D.; Shishkova, I.; Dobrev, D. *Thermal and Thermo-Catalytic Processes for Heavy Oil Conversion*; Marin Drinov Publishing House of Bulgarian Academy of Sciences: Sofia, Bulgaria, 2017; ISBN 978-954-322-892-8.
9. Stratiev, D.; Shishkova, I.; Dinkov, R.; Dobrev, D.; Argirov, G.; Yordanov, D. *The Synergy between Ebullated Bed Vacuum Residue Hydrocracking and Fluid Catalytic Cracking Processes in Modern Refining—Commercial Experience*; Professor Marin Drinov Publishing House of Bulgarian Academy of Sciences: Sofia, Bulgaria, 2022; ISBN 978-619-245-234-6.
10. Rodgers, R.P.; McKenna, A.M. Petroleum Analysis. *Anal. Chem.* **2011**, *83*, 4665–4687. [CrossRef]
11. Speight, J.G. *Handbook of Petroleum Product Analysis*, 2nd ed.; John Wiley & Sons: Hoboken, NJ, USA, 2015; ISBN 978-1-118-36926-5.
12. Moro, M.K.; dos Santos, F.D.; Folli, G.S.; Rom'ao, W.; Filgueiras, P.R. A review of chemometrics models to predict crude oil properties from nuclear magnetic resonance and infrared spectroscopy. *Fuel* **2021**, *303*, 121283. [CrossRef]
13. Shi, Q.; Wu, J. Review on Sulfur Compounds in Petroleum and Its Products: State-of-the-Art and Perspectives. *Energy Fuels* **2021**, *35*, 14445–14461. [CrossRef]
14. Lyu, W.; Zhang, L.; Li, K.; Wang, G.; Shi, Q.; Zhao, S.; Xu, C. Average Molecule Construction of Petroleum Fractions Based on ^{1}H-NMR. *AIChE J.* **2018**, *65*, 270–280. [CrossRef]
15. Yang, C.; Zhang, G.; Serhan, M.; Koivu, G.; Yang, Z.; Hollebone, B.; Lambert, P.; Brown, C.E. Characterization of naphthenic acids in crude oils and refined petroleum products. *Fuel* **2019**, *255*, 115849. [CrossRef]
16. Vieira, A.P.; Portela, N.A.; Neto, Á.C.; Lacerda, V., Jr.; Romão, W.; Castro, E.V.R.; Filgueiras, P.R. Determination of physicochemical properties of petroleum using 1H NMR spectroscopy combined with multivariate calibration. *Fuel* **2019**, *253*, 320–326. [CrossRef]
17. Hosseinifar, P.; Shahverdi, H. Development of a generalized model for predicting the composition of homologous groups derived from molecular type analyses to characterize petroleum fractions. *J. Pet. Sci. Eng.* **2021**, *204*, 108744. [CrossRef]
18. Chen, X.; Zhang, Y.; Han, J.; Zhang, L.; Zhao, S.; Xu, C.; Shi, Q. Direct Nickel Petroporphyrin Analysis through Electrochemical Oxidation in Electrospray Ionization Ultrahigh-Resolution Mass Spectrometry. *Energy Fuels* **2021**, *35*, 5748–5757. [CrossRef]
19. Maryutina, T.A.; Timerbaev, A.R. Metal speciation analysis of petroleum: Myth or reality? *Anal. Chim. Acta* **2017**, *991*, 1–8. [CrossRef] [PubMed]
20. Feng, S.; Cui, C.; Li, K.; Zhang, L.; Shi, Q.; Zhao, S.; Xu, C. Molecular composition modelling of petroleum fractions based on a hybrid structural unit and bond-electron matrix (SU-BEM) framework. *Chem. Eng. Sci.* **2019**, *201*, 145–156. [CrossRef]
21. Prado, G.H.C.; Rao, Y.; De Klerk, A. Nitrogen Removal from Oil: A Review. *Energy Fuels* **2017**, *31*, 14–36. [CrossRef]
22. Sama, S.G.; Barrère-Mangote, C.; Bouyssière, B.; Giusti, P.; Lobinski, R. Recent trends in element speciation analysis of crude oils and heavy petroleum fractions. *Trends Anal. Chem.* **2018**, *104*, 69–76. [CrossRef]
23. Dindoruk, B.; Ratnakar, R.R.; He, J. Review of recent advances in petroleum fluid properties and their representation. *J. Nat. Gas Sci. Eng.* **2020**, *83*, 103541. [CrossRef]

24. Rogel, E.; Hench, K.; Witt, M. Ultrahigh-Resolution Magnetic Resonance Mass Spectrometry Characterization of Crude Oil Fractions Obtained Using *n*-Pentane. *Energy Fuels* **2020**, *34*, 10773–10780. [CrossRef]
25. Solanki, P.; Baldaniya, D.; Jogani, D.; Chaudhary, B.; Shah, M.; Kshirsagar, A. Artificial intelligence: New age of transformation in petroleum upstream. *Pet. Res.* **2022**, *7*, 106–114. [CrossRef]
26. Stratiev, D.; Shishkova, I.; Tankov, I.; Pavlova, A. Challenges in characterization of residual oils. A review. *J. Pet. Sci. Eng.* **2019**, *178*, 227–250. [CrossRef]
27. Energy Intelligence Research. *The International Crude Oil Market Handbook*; Energy Intelligence: New York, NY, USA, 2006.
28. Alabdullah, M.A.; Gomez, A.R.; Vittenet, J.; Bendjeriou-Sedjerari, A.; Xu, W.; Abba, I.A.; Gascon, J. A Viewpoint on the Refinery of the Future: Catalyst and Process Challenges. *ACS Catal.* **2020**, *10*, 8131–8140. [CrossRef]
29. Al Jamri, M.; Li, J.; Smith, R. Molecular Modelling of Co-processing Biomass Fast Pyrolysis Oil in Fluid Catalytic Cracking Unit. *Ind. Eng. Chem. Res.* **2020**, *59*, 1989–2004. [CrossRef]
30. Ooms, A.C.; van den Berg, F.; Kapusta, S.D.; Nouwens, L.W. Processing opportunity crudes: A new strategy for crude selection. In Proceedings of the 2001 European Refining Technology Conference ERTC, Paris, France, 20 June 2001.
31. Qing, W. Processing high TAN crude: Part I. *Pet. Technol. Q.* **2010**, *4*, 35.
32. Swafford, P.; McCarthy, R. Improving crude oil selection. *PTQ Mag.* **2008**, *3*, 125–129.
33. Shishkova, I.; Stratiev, D.; Tavlieva, M.; Dinkov, R.; Yordanov, D.; Sotirov, S.; Sotirova, E.; Atanassova, V.; Ribagin, S.; Atanassov, K.; et al. Evaluation of the Different Compatibility Indices to Model and Predict Oil Colloidal Stability and Its Relation to Crude Oil Desalting. *Resources* **2021**, *10*, 75. [CrossRef]
34. Hernández, E.A.; Sánchez Reyna, G.; Ancheyta, J. Comparison of mixing rules based on binary interaction parameters for calculating viscosity of crude oil blends. *Fuel* **2019**, *249*, 198–205. [CrossRef]
35. Stratiev, D.; Shishkova, I.; Kolev, I.; Yordanov, D.; Toteva, V. Petroleum crude slate effect on H-Oil performance. *Int. J. Oil Gas Coal Technol.* **2021**, *28*, 3. [CrossRef]
36. Hsu, C.S.; Robinson, P.R. *Petroleum Science and Technology*; Springer: Berlin/Heidelberg, Germany, 2019.
37. Giles, H.N.; Mills, C.O. *Crude Oils: Their Sampling, Analysis, and Evaluation*; ASTM International: West Conshohocken, PA, USA, 2010.
38. Treese, S.A.; Pujado, P.R.; Jones, D.S.J. *Handbook of Petroleum Processing*, 2nd ed.; Springer: Cham, Switzerland, 2015.
39. Abdel-AalMohammed, H.K.; Alsahlawi, A. *Petroleum Economics and Engineering*, 3rd ed.; Taylor & Francis Group: Abingdon, UK, 2014.
40. Chang, A.; Pashikanti, K.; Liu, Y.A. *Refinery Engineering. Integrated Process Modeling and Optimization*; Wiley-VCH Verlag & Co. KGaA: Weinheim, Germany, 2012.
41. Speight, J. *Rules of Thumb for Petroleum Engineers*; John Wiley & Sons, Inc.: Hoboken, NJ, USA, 2017.
42. Tissot, B.P.; Welte, D.H. *Petroleum Formation and Occurrence*, 2nd ed.; Springer: New York, NY, USA, 1984; p. 699.
43. Younes, M.A.; Afife, M.M.; El Nady, M.M. Geochemical characteristics of crude oils dependent specific and biomarker distributions in the central-southern Gulf of Suez, Egypt, Part A: Recovery, Utilization, and Environmental Effects. *Energy Sources* **2017**, *39*, 191–200. [CrossRef]
44. Gray, A.C.; Richard, J.D.; Robert, A.S.; Henery, I.H. Organic geochemistry and oil—Source correlations, Paleozoic of Ohio. *AAPG Bull.* **1987**, *71*, 788–809.
45. Rønningsen, H. Prediction of viscosity and surface tension of North sea petroleum fluids by using the average molecular weight. *Energy Fuels* **1993**, *7*, 565–573. [CrossRef]
46. Hinkle, A.; Shin, E.J.; Liberatore, M.W.; Herring, A.M.; Batzle, M. Correlating the chemical and physical properties of a set of heavy oils from around the world. *Fuel* **2008**, *87*, 3065–3070. [CrossRef]
47. Sinha, U.; Dindoruk, B.; Soliman, M.Y. Physics Augmented Correlations and Machine Learning Methods to Accurately Calculate Dead Oil Viscosity Based on the Available Inputs. *SPE J.* **2022**, *27*, 3240–3253. [CrossRef]
48. Yarranton, H.W. Estimation of SARA fraction properties with the SRK EOS. *J. Can. Pet. Technol* **2004**, *43*, 9.
49. Goossens, A.G. Prediction of Molecular Weight of Petroleum Fractions. *Ind. Eng. Chem. Res.* **1996**, *35*, 985–988. [CrossRef]
50. Stratiev, D.; Dinkov, R.; Kirilov, K.; Petkov, K. Method calculates crude properties. *Oil Gas J.* **2008**, *106*, 48–52.
51. Stratiev, D.; Shishkova, I.; Nikolaychuk, E.; Atanasova, V.; Atanassov, K. Investigation of relations of properties of straight run and H-Oil unconverted vacuum residual oils. *Pet Coal* **2019**, *61*, 763–776.
52. Carbognani, L.; Carbognani-Arambarri, L.; Lopez-Linares, F.; Pereira-Almao, P. Suitable Density Determination for Heavy Hydrocarbons by Solution Pycnometry: Virgin and Thermal Cracked Athabasca Vacuum Residue Fractions. *Energy Fuels* **2011**, *25*, 3663–3670. [CrossRef]
53. Zhao, H.; Memon, A.; Gao, J.; Taylor, S.D.; Sieben, D.; Ratulowski, J.; Alboudwarej, H.; Pappas, J.; Creek, J. Heavy Oil Viscosity Measurements: Best Practices and Guidelines. *Energy Fuels* **2016**, *30*, 5277–5290. [CrossRef]
54. Stratiev, D.; Shishkova, I.; Dinkov, R.; Kolev, I.; Argirov, G.; Ivanov, V.; Ribagin, S.; Atanassova, V.; Atanassov, K.; Stratiev, D.; et al. Intercriteria Analysis to Diagnose the Reasons for Increased Fouling in a Commercial Ebullated Bed Vacuum Residue Hydrocracker. *ACS Omega* **2022**, *7*, 30462–30476. [CrossRef]
55. Hosseinifar, P.; Shahverdi, H. A predictive method for constructing the distillation curve of petroleum fluids using their physical bulk properties. *J. Pet. Sci. Eng.* **2021**, *200*, 108403. [CrossRef]
56. Diaz, O.C.; Yarranton, H.W. Applicability of Simulated Distillation for Heavy Oils. *Energy Fuels* **2019**, *33*, 6083–6087. [CrossRef]
57. Santos, R.N.G.; Lima, E.R.A.; Paredes, M.L.L. ASTM D86 distillation curve: Experimental analysis and premises for literature modeling. *Fuel* **2021**, *284*, 118958. [CrossRef]

58. Austrich, A.J.; Buenrostro-González, E.; Lira-Galeana, C. ASTM D-5307 and ASTM D-7169 SIMDIS Standards: A Comparison and Correlation of Methods. *Pet. Sci. Technol.* **2015**, *33*, 657–663. [CrossRef]
59. Reiter, A.M.; Wallek, T.; Mair-Zelenka, P.; Siebenhofer, M.; Reinberger, P. Characterization of Crude Oil by Real Component Surrogates. *Energy Fuels* **2014**, *28*, 5565–5571. [CrossRef]
60. Azinfar, B.; Zirrahi, M.; Hassanzadeh, H.; Abedi, J. Characterization of heavy crude oils and residues using combined Gel Permeation Chromatography and simulated distillation. *Fuel* **2018**, *233*, 885–893. [CrossRef]
61. Behrenbruch, P.; Dedigama, T. Classification and characterisation of crude oils based on distillation properties. *J. Pet. Sci. Eng.* **2007**, *57*, 166–180. [CrossRef]
62. Sánchez, S.; Ancheyta, J.; McCaffrey, W.C. Comparison of Probability Distribution Functions for Fitting Distillation Curves of Petroleum. *Energy Fuels* **2007**, *21*, 2955–2963. [CrossRef]
63. Rodrigues, V.; Silva, S.R.; Romão, W.; Castro, E.V.; Filgueiras, P.R. Determination of crude oil physicochemical properties by high-temperature gas chromatography associated with multivariate calibration. *Fuel* **2018**, *220*, 389–395. [CrossRef]
64. Nascimento, M.H.; Oliveira, B.P.; Rainha, K.P.; Castro, E.V.; Silva, S.R.; Filgueiras, P.R. Determination of flash point and Reid vapor pressure in petroleum from HTGC and DHA associated with chemometrics. *Fuel* **2018**, *234*, 643–649. [CrossRef]
65. Giordano, G.F.; Vieira, L.C.; Gomes, A.O.; de Carvalho, R.M.; Kubota, L.T.; Fazzio, A.; Schleder, G.R.; Gobbi, A.L.; Lima, R.S. Distilling small volumes of crude oil. *Fuel* **2021**, *285*, 119072. [CrossRef]
66. Gómez-Siurana, A.; Font-Escamilla, A.; García-Soler, C. Learning about distillation curves as a way to define a process stream from crude petroleum. *Educ. Chem. Eng.* **2018**, *26*, 35–40. [CrossRef]
67. Nalinakshan, S.; Sivasubramanian, V.; Ravi, V.; Vasudevan, A.; Sankar, M.R.; Arunachalam, K. Progressive crude oil distillation: An energy-efficient alternative to conventional distillation process. *Fuel* **2019**, *239*, 1331–1337. [CrossRef]
68. Behrooz, H.A. Robust set-point optimization of inferential control system of crude oil distillation units. *ISA Trans.* **2019**, *95*, 93–109. [CrossRef] [PubMed]
69. Espinosa-Peña, M.; Figueroa-Gómez, Y.; Jiménez-Cruz, F. Simulated Distillation Yield Curves in Heavy Crude Oils: A Comparison of Precision between ASTM D-5307 and ASTM D-2892 Physical Distillation. *Energy Fuels* **2004**, *18*, 1832–1840. [CrossRef]
70. Coutinho, D.M.; França, D.; Vanini, G.; Gomes, A.O.; Azevedo, D.A. Understanding the molecular composition of petroleum and its distillation cuts. *Fuel* **2022**, *311*, 122594. [CrossRef]
71. Meirelles, L.B.; Menechini, P.; Chrisman, E.C.A.N.; Ndiaye, P.M. Comparison of The Experimental TBP Curve with Results of Empirical Correlations And Commercial Simulators. *Quest J. J. Softw. Eng. Simul.* **2017**, *3*, 1–5.
72. Kadiev, K.M.; Gagarin, S.G.; Oknina, N.V.; Kadieva, M.K.; Batov, A.E. Mathematical Description of Fractioning Curves as a Basis for Balance Modeling of Oil Feedstock Refining Processes. *Glob. J. Pure Appl. Math.* **2016**, *12*, 4553–4568.
73. Nedelchev, A.; Stratiev, D.; Ivanov, A.; Stoilov, G. Boiling Point Distribution Of Crude Oils Based On TBP And ASTM D-86 Distillation Data. *Pet. Coal* **2011**, *53*, 275–290.
74. Stratiev, D.; Nedelchev, A.; Dinkov, R.; Batchvarov, A. It's possible to derive TBP from partial distillation data. *Oil Gas J.* **2011**, *109*, 114–122.
75. Stratiev, D.S.; Marinov, I.; Nedelchev, A.; Velkov, I.; Stratiev, D.D.; Veli, A.; Mitkova, M.; Stanulov, K. Evaluation of approaches for conversion of ASTM into TBP distillation data of oil fractions. *Oil Gas Eur. Mag.* **2014**, *4*, 216–221.
76. Nikolaychuk, E.; Stratiev, D.; Velkov, I.; Veli, A.; Sotirov, S.; Mitkova, M. Conversion of heavy oil distillation data from ASTM D-1160 to ASTM D-5236. *Pet. Coal* **2015**, *57*, 266–279.
77. Nikolaychuk, E.; Stratiev, D.; Shishkova, I.; Veli, A.; Mitkova, M.; Yordanov, D. Investigation On Feasibility To Simulate Crude Oil True Boiling Point Distillation By Application Of ASTM D-7169 Simulated Distillation And Combination Of ASTM D-86 And ASTM D-1160 Physical Distillation Methods. *Pet. Coal* **2016**, *58*, 194–208.
78. Nikolaychuck, E.; Veli, A.; Stratiev, D.; Shishkova, I.; Burilkova, A.; Tamahkiarova, E.; Mitkova, M.; Yordanov, D. Physical Vacuum Distillation and High Temperature Simulated Distillation of Residual Oils from Different Origin. *Int. J. Oil Gas Coal Technol.* **2018**, *17*, 209–221. [CrossRef]
79. Hsu, C.S.; Robinson, P.R. *Springer Handbook of Petroleum Technology*; Springer: Berlin/Heidelberg, Germany, 2017.
80. Liñan, L.Z.; Lima, N.N.; Manenti, F.; Maciel, M.W.; Filho, R.M.; Medina, L. Experimental campaign, modeling, and sensitivity analysis for the molecular distillation of petroleum residues 673.15K+. *Chem. Eng. Res. Des.* **2012**, *90*, 243–258. [CrossRef]
81. Liñan, L.Z.; Lima, N.M.N.; Maciel, M.R.W.; Filho, R.M.; Medina, L.C.; Embiruçu, M. Correlation for predicting the molecular weight of Brazilian petroleum residues and cuts: An application for the simulation of a molecular distillation process. *J. Pet. Sci. Eng.* **2011**, *78*, 78–85. [CrossRef]
82. Rodriguez, A.L.C.; Tovar, L.P.; Maciel, M.R.W.; Filho, R.M. Optimizing the Polynomial to Represent the Extended True Boiling Point Curve from High Vacuum Distillation Data Using Genetic Algorithms. *Chem. Eng. Trans.* **2015**, *43*, 1561–1566. [CrossRef]
83. Sbaite, P.; Batistella, C.B.; Winter, A.; Vasconcelos, C.J.G.; Maciel, M.R.W.; Filho, R.M.; Gomes, A.; Medina, L.; Kunert, R. True Boiling Point Extended Curve of Vacuum Residue Through Molecular Distillation. *Pet. Sci. Technol.* **2006**, *24*, 265–274. [CrossRef]
84. Haynes, H.W.; Matthews, M.A. Continuous-Mixture Vapor-Liquid Equilibria Computations Based on True Boiling Point Distillations. *Ind. Eng. Chem. Res.* **1991**, *30*, 1911–1915. [CrossRef]
85. Lopes, M.S.; Watanabe, E.R.L.D.R.; Lopes, E.S.; Gomes, V.M.; Medina, L.C.; Filho, R.M.; Maciel, M.R.W. Extending the true boiling point curve of a heavy crude oil by means of molecular distillation and characterization of the products obtained. *Pet. Sci. Technol.* **2017**, *35*, 1523–1529. [CrossRef]

86. Lopes, M.; Filho, R.M.; Maciel, M.R.W.; Medina, L. Extension of the TBP Curve of Petroleum Using the Correlation DESTMOL. *Procedia Eng.* **2012**, *42*, 726–732. [CrossRef]
87. Meirelles, L.B.; Chrisman, E.C.A.N.; de Andrade, F.B.; de Oliveira, L.C.M. Comparison of the Distillation Curve Obtained Experimentally with the Curve Extrapolated by a Commercial Simulator. *World Acad. Sci. Eng. Technol. Int. J. Chem. Mol. Eng.* **2017**, *11*, 260–264. [CrossRef]
88. Xavier, G.M.; Boaventura, K.M.; Peixoto, F.C. On The Use of Continuous Distribution Models For Characterization Of Crude Oils. *Lat. Am. Appl. Res.* **2011**, *41*, 325–329.
89. Hosseinifar, P.; Shahverdi, H. Prediction of the ASTM and TBP distillation curves and specific gravity distribution curve for fuels and petroleum fluids. *Can. J. Chem. Eng.* **2021**, *100*, 3288–3310. [CrossRef]
90. Kotzakoulakis, K.; George, S.C. A simple and flexible correlation for predicting the viscosity of crude oils. *J. Pet. Sci. Eng.* **2017**, *158*, 416–423. [CrossRef]
91. Boduszynski, M.M. Composition of heavy petroleums. 2. Molecular characterization. *Energy Fuels* **1988**, *2*, 597–613. [CrossRef]
92. Hao, J.; Che, Y.; Tian, Y.; Li, D.; Zhang, J.; Qiao, Y. Thermal Cracking Characteristics and Kinetics of Oil Sand Bitumen and Its SARA Fractions by TG–FTIR. *Energy Fuels* **2017**, *31*, 1295–1309. [CrossRef]
93. Redelius, P.; Soenen, H. Relation between bitumen chemistry and performance. *Fuel* **2015**, *140*, 34–43. [CrossRef]
94. Le Guern, M.; Chailleux, E.; Farcas, F.; Dreessen, S.; Mabille, I. Physico-chemical analysis of five hard bitumens: Identification of chemical species and molecular organization before and after artificial aging. *Fuel* **2010**, *89*, 3330–3339. [CrossRef]
95. Lesueur, D. The colloidal structure of bitumen: Consequences on the rheology and on the mechanisms of bitumen modification. *Adv. Colloid Interface Sci.* **2009**, *145*, 42–82. [CrossRef]
96. Keshmirizadeh, E.; Shobeirian, S.; Memariani, M. Determination of saturates, aromatics, resins and asphaltenes (SARA) fractions in Iran crude oil sample with chromatography methods: Study of the geochemical parameters. *J. Appl. Chem. Res.* **2013**, *7*, 15–24.
97. Kharrat, A.M.; Zacharia, J.; Cherian, V.J.; Anyatonwu, A. Issues with Comparing SARA Methodologies. *Energy Fuels* **2007**, *21*, 3618–3621. [CrossRef]
98. Fan, T.; Buckley, J.S. Rapid and Accurate SARA Analysis of Medium Gravity Crude Oils. *Energy Fuels* **2002**, *16*, 1571–1575. [CrossRef]
99. Ashoori, S.; Sharifi, M.; Masoumi, M.; Salehi, M.M. The relationship between SARA fractions and crude oil stability. *Egypt. J. Pet.* **2017**, *26*, 209–213. [CrossRef]
100. Reyes-Gonzalez, D.; Ramirez-Jaramillo, E.; Manero, O.; Lira-Galeana, C.; del Rio, J.M. Estimation of the SARA Composition of Crude Oils from Bubblepoint Pressure Data. *Energy Fuels* **2016**, *30*, 6913–6922. [CrossRef]
101. Rudyk, S. Relationships between SARA fractions of conventional oil, heavy oil, natural bitumen and residues. *Fuel* **2018**, *216*, 330–340. [CrossRef]
102. Abutaqiya, M.I.L.; Sisco, C.J.; Khemka, Y.; Safa, M.A.; Ghloum, E.F.; Rashed, A.M.; Gharbi, R.; Santhanagopalan, S.; Al-Qahtani, M.; Al-Kandari, E.; et al. Accurate Modeling of Asphaltene Onset Pressure in Crude Oils Under Gas Injection Using Peng–Robinson Equation of State. *Energy Fuels* **2020**, *34*, 4055–4070. [CrossRef]
103. Ting, P.D.; Hirasaki, G.J.; Chapman, W. Modeling of Asphaltene Phase Behavior with the SAFT Equation of State. *Pet. Sci. Technol.* **2003**, *21*, 647–661. [CrossRef]
104. Panuganti, S.R.; Vargas, F.M.; Gonzalez, D.L.; Kurup, A.S.; Chapman, W.G. PC-SAFT characterization of crude oils and modeling of asphaltene phase behavior. *Fuel* **2012**, *93*, 658–669. [CrossRef]
105. Punnapala, S.; Vargas, F.M. Revisiting the PC-SAFT characterization procedure for an improved asphaltene precipitation prediction. *Fuel* **2013**, *108*, 417–429. [CrossRef]
106. Abutaqiya, M.I.L.; Sisco, C.J.; Wang, J.; Vargas, F.M. Systematic Investigation of Asphaltene Deposition in the Wellbore and Near-Wellbore Region of a Deepwater Oil Reservoir Under Gas Injection. Part 1: Thermodynamic Modeling of the Phase Behavior of Polydisperse Asphaltenes. *Energy Fuels* **2019**, *33*, 3632–3644. [CrossRef]
107. Sisco, C.J.; Abutaqiya, M.I.L.; Wang, F.; Zhang, J.; Tavakkoli, M.; Vargas, F.M. Asphaltene Precipitation Modeling. In *Asphaltene Deposition: Fundamentals, Prediction, Prevention, and Remediation*, 1st ed.; CRC Press: Boca Raton, FL, USA, 2018; pp. 111–159. [CrossRef]
108. Xu, C.; Gao, J.; Zhao, S.; Lin, S. Correlation between feedstock SARA components and FCC product yields. *Fuel* **2005**, *84*, 669–674. [CrossRef]
109. Fukuyama, H.; Terai, S. Kinetic Study on the Hydrocracking Reaction of Vacuum Residue Using a Lumping Model. *Pet. Sci. Technol.* **2007**, *25*, 277–287. [CrossRef]
110. Stratiev, D.; Dinkov, R.; Shishkova, I.; Sharafutdinov, I.; Ivanova, N.; Mitkova, M.; Yordanov, D.; Rudnev, N.; Stanulov, K.; Artemiev, A.; et al. What is Behind the High Values of Hot Filtration Test of the Ebullated Bed Residue H-Oil Hydrocracker Residual Oils? *Energy Fuels* **2016**, *30*, 7037–7054. [CrossRef]
111. Fals, J.; García, J.R.; Falco, M.; Sedran, U. Coke from SARA fractions in VGO. Impact on Y zeolite acidity and physical properties. *Fuel* **2018**, *225*, 26–34. [CrossRef]
112. Pujro, R.; Falco, M.; Devard, A.; Sedran, U. Reactivity of the saturated, aromatic and resin fractions of ATR resids under FCC conditions. *Fuel* **2014**, *119*, 219–225. [CrossRef]
113. Stratiev, D.; Minkov, D.; Haas, A. Removal of coke precursors—Influence on FCC yield distribution. *Erdol Erdgas Kohle* **1997**, *113*, 436–439.

114. Hauser, A.; AlHumaidan, F.; Al-Rabiah, H.; Halabi, M.A. Study on Thermal Cracking of Kuwaiti Heavy Oil (Vacuum Residue) and Its SARA Fractions by NMR Spectroscopy. *Energy Fuels* **2014**, *28*, 4321–4332. [CrossRef]
115. Haitao, S.; Guofeng, J.; Xinyi, Z.; Xiang, Z.; Yuxia, Z.; Zhijian, D. Hydrocarbon composition of different VGO feedstocks and its correlation with FCC product distribution. *China Pet. Process. PE* **2013**, *15*, 32–39.
116. Fortain, P.D. Étude de la Réactivité Des Résidus Pétroliers en Hydroconversion. Ph.D. Thesis, Université Bordeaux, Bordeaux, France, 2010. Available online: https://core.ac.uk/download/pdf/52311285.pdf (accessed on 10 September 2022).
117. Félix, G.; Ancheyta, J. Comparison of hydrocracking kinetic models based on SARA fractions obtained in slurry-phase reactor. *Fuel* **2019**, *241*, 495–505. [CrossRef]
118. Santos, D.C.; Filipakis, S.D.; Rolemberg, M.P.; Lima, E.R.; Paredes, M.L. Asphaltene flocculation parameter in Brazilian crude oils and synthetic polar and nonpolar mixtures: Experimental and modeling. *Fuel* **2017**, *199*, 606–615. [CrossRef]
119. Sanchez-Minero, F.; Ancheyta, J.; Silva-Oliver, G.; Flores-Valle, S. Predicting SARA composition of crude oil by means of NMR. *Fuel* **2013**, *110*, 318–321. [CrossRef]
120. Aske, N.; Kallevik, H.; Sjo'blom, J. Determination of Saturate, Aromatic, Resin, and Asphaltenic (SARA) Components in Crude Oils by Means of Infrared and Near-Infrared Spectroscopy. *Energy Fuels* **2001**, *15*, 1304–1312. [CrossRef]
121. Sieben, V.J.; Stickel, A.J.; Obiosa-Maife, C.; Rowbotham, J.; Memon, A.; Hamed, N.; Ratulowski, J.; Mostowfi, F. Optical Measurement of Saturates, Aromatics, Resins, And Asphaltenes in Crude Oil. *Energy Fuels* **2017**, *31*, 3684–3697. [CrossRef]
122. Fan, T.; Wang, J.; Buckley, J.S. Evaluating crude oils by SARA analysis. In Proceedings of the SPE/DOE Improved Oil Recovery Symposium, Tulsa, Oklahoma, 13–17 April 2002. [CrossRef]
123. Sinnathambi, C.M.; Mohamad-Nor, N. Relationship Between SARA Fractions and Crude Oil Fouling. *J. Appl. Sci.* **2012**, *12*, 2479–2483. [CrossRef]
124. Zhang, J.; Tian, Y.; Qiao, Y.; Yang, C.; Shan, H. Structure and reactivity of Iranian vacuum residue and its eight group-fractions. *Energy Fuels.* **2017**, *31*, 8072–8086. [CrossRef]
125. Hénaut, G.I.; Barré, L.; Argillier, J.F. Heavy Oil Dilution. *Oil Gas Sci. Technol. Rev. IFP* **2004**, *59*, 503–509.
126. Brough, S.A.; Riley, S.H.; Sean McGrady, G.; Tanhawiriyakul, S.; Romero-Zero, L.; Willson, C.D. Low temperature extraction and upgrading of oil sands and bitumen in supercritical fluid mixtures. *Chem. Commun.* **2010**, *46*, 4923–4925. [CrossRef]
127. Akbarzadeh, K.; Dhillon, A.; Svrcek, A.W.Y.; Yarranton, H.W. Methodology for the Characterization and Modeling of Asphaltene Precipitation from Heavy Oils Diluted with *n*-Alkanes. *Energy Fuels* **2004**, *18*, 1434–1441. [CrossRef]
128. Guzmán, R.; Ancheyta, J.; Trejo, F.; Rodríguez, S. Methods for determining asphaltene stability in crude oils. *Fuel* **2017**, *188*, 530–543. [CrossRef]
129. Xiong, R.; Guo, J.; Kiyingi, W.; Feng, H.; Sun, T.; Yang, X.; Li, Q. Method for Judging the Stability of Asphaltenes in Crude Oil. *ACS Omega* **2020**, *5*, 21420–21427. [CrossRef]
130. Abeed, Q.; Leythaeuser, D.; Littke, R. Geochemistry, origin and correlation of crude oils in Lower Cretaceous sedimentary sequences of the southern Mesopotamian Basin, southern Iraq. *Org. Geochem.* **2012**, *46*, 113–126. [CrossRef]
131. Kumar, R.; Maheshwari, S.; Voolapalli, R.K.; Upadhyayula, S. Investigation of physical parameters of crude oils and their impact on kinematic viscosity of vacuum residue and heavy product blends for crude oil selection. *J. Taiwan Inst. Chem. Eng.* **2021**, *120*, 33–42. [CrossRef]
132. Coronel-García, M.; de la Torre, A.R.; Domínguez-Esquivel, J.; Melo-Banda, J.; Martínez-Salazar, A. Heavy oil hydrocracking kinetics with nano-nickel dispersed in PEG300 as slurry phase catalyst using batch reactor. *Fuel* **2021**, *283*, 118930. [CrossRef]
133. Buckley, J.; Morrow, N. *Wettability and Imbibition: Microscopic Distribution of Wetting and its Consequences at the Core and Field Scales*; New Mexico Petroleum Recovery Research Center: Soccoro, NM, USA, 2003. [CrossRef]
134. Hemmingsen, P.V.; Silset, A.; Hannisdal, A.; Sjblom, J. Emulsions of Heavy Crude Oils. I: Influence of Viscosity, Temperature, and Dilution. *J. Dispers. Sci. Technol.* **2005**, *26*, 615–627. [CrossRef]
135. Stratiev, D.; Nenov, S.; Shishkova, I.; Georgiev, B.; Argirov, G.; Dinkov, R.; Yordanov, D.; Atanassova, V.; Vassilev, P.; Atanassov, K. Commercial Investigation of the Ebullated-Bed Vacuum Residue Hydrocracking in the Conversion Range of 55–93%. *ACS Omega* **2020**, *5*, 33290–33304. [CrossRef] [PubMed]
136. Youtcheff, J. *Automated High-Performance Liquid Chromatography Saturate, Aromatic, Resin, and Asphaltene Separation. Technical Report FHWA-HRT-15-055*; Turner-Fairbank Highway Research Center: McLean, VA, USA, 2016.
137. Yarranton, H. Prediction of Crude Oil Saturate Content from a SimDist Assay. *Energy Fuels* **2022**, *36*, 8809–8817. [CrossRef]
138. Stratiev, D.; Shishkova, I.; Dinkov, R.; Petrov, I.; Kolev, I.; Yordanov, D.; Sotirov, S.; Sotirova, E.; Atanassova, V.; Ribagin, S.; et al. Empirical Models to Characterize the Structural and Physiochemical Properties of Vacuum Gas Oils with Different Saturate Contents. *Resources* **2021**, *10*, 71. [CrossRef]
139. Abutaqiya, M. Advances in Thermodynamic Modeling of Nonpolar Hydrocarbons and Asphaltene Precipitation in Crude Oils. Ph.D. Thesis, Rice University, Houston, TX, USA, 2019.
140. Abutaqiya, M.I.L.; Alhammadi, A.A.; Sisco, C.J.; Vargas, F.M. Aromatic Ring Index (ARI): A Characterization Factor for Nonpolar Hydrocarbons from Molecular Weight and Refractive Index. *Energy Fuels* **2021**, *35*, 1113–1119. [CrossRef]
141. Stratiev, D.S.; Marinov, I.M.; Shishkova, I.K.; Dinkov, R.K.; Stratiev, D.D. Investigation on feasibility to predict the content of saturate plus mono-nuclear aromatic hydrocarbons in vacuum gas oils from bulk properties and empirical correlations. *Fuel* **2014**, *129*, 156–162. [CrossRef]

142. Sharafutdinov, I.; Stratiev, D.; Shishkova, I.; Dinkov, R.; Pavlova, A.; Petkov, P.; Rudnev, N. Dependence of cetane index on aromatic content in diesel fuels. *OGEM* **2012**, *38*, 148–152.
143. Marshall, A.G.; Rodgers, R.P. Petroleomics: The Next Grand Challenge for Chemical Analysis. *Accounts Chem. Res.* **2004**, *37*, 53–59. [CrossRef]
144. Niyonsaba, E.; Manheim, J.M.; Yerabolu, R.; Kenttämaa, H.I. Recent Advances in Petroleum Analysis by Mass Spectrometry. *Anal. Chem.* **2018**, *91*, 156–177. [CrossRef] [PubMed]
145. Huynh, K.; Jensen, A.; Sundberg, J. Extended characterization of petroleum aromatics using off-line LC-GCMS. *PeerJ Anal. Chem.* **2021**, *3*, e12. [CrossRef]
146. Angolini, C.F.; Pudenzi, M.A.; Batezelli, A.; Eberlin, M.N. *Comprehensive Petroleomics: Multiple Mass Spectrometry Strategies for Crude Oil Characterization*; John Wiley & Sons, Inc.: Hoboken, NJ, USA, 2017; pp. 1–16. [CrossRef]
147. Efimov, I.; Povarov, V.G.; Rudko, V.A. Comparison of UNIFAC and LSER Models for Calculating Partition Coefficients in the Hexane–Acetonitrile System Using Middle Distillate Petroleum Products as an Example. *Ind. Eng. Chem. Res.* **2022**, *61*, 9575–9585. [CrossRef]
148. Smyshlyaeva, K.I.; Rudko, V.A.; Kuzmin, K.A.; Povarov, V.G. Asphaltene genesis influence on the low-sulfur residual marine fuel sedimentation stability. *Fuel* **2022**, *328*, 125291. [CrossRef]
149. Käfer, U.; Gröger, T.M.; Rohbogner, C.J.; Struckmeier, D.; Saraji-Bozorgzad, M.R.; Wilharm, T.; Zimmermann, R. Detailed Chemical Characterization of Bunker Fuels by High-Resolution Time-of-Flight Mass Spectrometry Hyphenated to GC × GC and Thermal Analysis. *Energy Fuels* **2019**, *33*, 10745–10755. [CrossRef]
150. Saitova, A.; Strokin, S.; Ancheyta, J. Evaluation and comparison of thermodynamic and kinetic parameters for oxidation and pyrolysis of Yarega heavy crude oil asphaltenes. *Fuel* **2021**, *297*, 120703. [CrossRef]
151. Qian, K.; Mennito, A.S.; Edwards, K.E.; Ferrughelli, D.T. Observation of vanadyl porphyrins and sulfur-containing vanadyl porphyrins in a petroleum asphaltene by atmospheric pressure photonionization Fourier transform ion cyclotron resonance mass spectrometry. *Rapid Commun. Mass Spectrom.* **2008**, *22*, 2153–2160. [CrossRef]
152. Li, H.; Li, S.; Wu, J.; Xie, L.; Liang, Y.; Zhang, Y.; Zhao, S.; Xu, C.; Shi, Q. Molecular characterization of aromatics in petroleum fractions by combining silica sulfuric acid sulfonation with electrospray ionization high-resolution mass spectrometry. *Fuel* **2022**, *317*, 123463. [CrossRef]
153. Shi, Q.; Hou, D.; Chung, K.H.; Xu, C.; Zhao, S.; Zhang, Y. Characterization of Heteroatom Compounds in a Crude Oil and Its Saturates, Aromatics, Resins, and Asphaltenes (SARA) and Non-basic Nitrogen Fractions Analyzed by Negative-Ion Electrospray Ionization Fourier Transform Ion Cyclotron Resonance Mass Spectrometry. *Energy Fuels* **2010**, *24*, 2545–2553. [CrossRef]
154. Panda, S.; Alawani, N.; Lajami, A.; Al-Qunaysi, T.; Muller, H. Characterization of aromatic hydrocarbons and sulfur heterocycles in Saudi Arabian heavy crude oil by gel permeation chromatography and ultrahigh resolution mass spectrometry. *Fuel* **2019**, *235*, 1420–1426. [CrossRef]
155. Shi, Q. Distribution of acids and neutral nitrogen compounds in a Chinese crude oil and its fractions: Characterized by negative-ion electrospray ionization Fourier transform ion cyclotron resonance mass spectrometry. *Energy Fuels* **2010**, *24*, 4005–4011. [CrossRef]
156. Wu, Q.; Pomerantz, A.E.; Mullins, O.C.; Zare, R.N. Laser-Based Mass Spectrometric Determination of Aggregation Numbers for Petroleum- and Coal-Derived Asphaltenes. *Energy Fuels* **2014**, *28*, 475–482. [CrossRef]
157. Wu, Z.; Rodgers, R.P.; Marshall, A.G. Two- and Three- Dimensional van Krevelen Diagrams: A Graphical Analysis Complementary to the Kendrick Mass Plot for Sorting Elemental Compositions of Complex Organic Mixtures Based on Ultrahigh-Resolution Broadband Fourier Transform Ion Cyclotron Resonance Mass Measurements. *Anal. Chem.* **2004**, *76*, 2511–2516. [PubMed]
158. Bava, Y.; Geronés, M.; Giovanetti, L.; Andrini, L.; Erben, M. Speciation of sulphur in asphaltenes and resins from Argentinian petroleum by using XANES spectroscopy. *Fuel* **2019**, *256*, 115952. [CrossRef]
159. Ehiosun, K.; Grimaud, R.; Lobinski, R. Mass spectrometric analysis for carboxylic acids as viable markers of petroleum hydrocarbon biodegradation. *Trends Environ. Anal. Chem.* **2022**, *35*, e00172. [CrossRef]
160. Zhu, Y.; Guo, Y.; Teng, H.; Liu, J.; Tian, F.; Cui, L.; Li, W.; Liu, J.; Wang, C.; Li, D. Analysis of oxygen-containing species in coal tar by comprehensive two-dimensional GC×GC-TOF and ESI FT-ICR mass spectrometry through a new subfraction separation method. *J. Energy Inst.* **2022**, *101*, 209–220. [CrossRef]
161. Porto, C.; Pinto, F.; Souza, L.; Madeira, N.; Neto, Á.; de Menezes, S.; Chinelatto, L., Jr.; Freitas, C.; Vaz, B.; Lacerda, V., Jr.; et al. Characterization of organosulfur compounds in asphalt cement samples by ESI(+)FT-ICR MS and 13C NMR spectroscopy. *Fuel* **2019**, *256*, 115923. [CrossRef]
162. Qian, K. Molecular Characterization of Heavy Petroleum by Mass Spectrometry and Related Techniques. *Energy Fuels* **2021**, *35*, 18008–18018. [CrossRef]
163. Mullins, O.C.; Sheu, E.Y.; Hammami, A.; Marshall, A.G. *Asphaltenes, Heavy Oils, and Petroleomics*; Springer: Berlin/Heidelberg, Germany, 2007.
164. Pabón, R.E.C.; Filho, C.R.D.S. Crude oil spectral signatures and empirical models to derive API gravity. *Fuel* **2019**, *237*, 1119–1131. [CrossRef]
165. Pinkston, D.S.; Duan, P.; Gallardo, V.A.; Habicht, S.C.; Tan, X.; Qian, K.; Gray, M.; Müllen, K.; Kenttämaa, H.I. Analysis of Asphaltenes and Asphaltene Model Compounds by Laser-Induced Acoustic Desorption/Fourier Transform Ion Cyclotron Resonance Mass Spectrometry. *Energy Fuels* **2009**, *23*, 5564–5570. [CrossRef]

166. Bissada, K.K.; Tan, J.; Szymczyk, E.; Darnell, M.; Mei, M. Group-type characterization of crude oil and bitumen. Part I: Enhanced separation and quantification of saturates, aromatics, resins and asphaltenes (SARA). *Org. Geochem.* **2016**, *95*, 21–28. [CrossRef]
167. Bissada, K.K.; Tan, J.; Szymezyk, E.; Darnell, M.; Mei, M. Group-Type Characterization of Crude Oil and Bitumen. Part II: Efficient Separation and Quantification of Normal-Paraffins Iso-Paraffins and Naphthenes (PIN). *Fuel* **2016**, *173*, 217–221. [CrossRef]
168. Robson, W.J.; Sutton, P.A.; McCormack, P.; Chilcott, N.P.; Rowland, S.J. Class Type Separation of the Polar and Apolar Components of Petroleum. *Anal. Chem.* **2017**, *89*, 2919–2927. [CrossRef] [PubMed]
169. Robbins, W.K. Quantitative Measurement of Mass and Aromaticity Distributions for Heavy Distillates 1. Capabilities of the HPLC-2 System. *J. Chromatogr. Sci.* **1998**, *36*, 457–466. [CrossRef]
170. Putman, J.C.; Rowland, S.M.; Podgorski, D.C.; Robbins, W.K.; Rodgers, R.P. Dual-Column Aromatic Ring Class Separation with Improved Universal Detection across Mobile-Phase Gradients via Eluate Dilution. *Energy Fuels* **2017**, *31*, 12064–12071. [CrossRef]
171. Giraldo-Dávila, D.; Chacón-Patiño, M.L.; Orrego-Ruiz, J.A.; Blanco-Tirado, C.; Combariza, M.Y. Improving Compositional Space Accessibility in (+) APPI FT-ICR Mass Spectrometric Analysis of Crude Oils by Extrography and Column Chromatography Fractionation. *Fuel* **2016**, *185*, 45–58. [CrossRef]
172. Chawla, B.H.; Bryan, E.; Green, L.A.; Di Sanzo, F.P. Fractionation of De-Asphalted Oil of Vacuum Resid Using Preparative High Performance Liquid Chromatographic Separations. U.S. Patent US20130055795A1, 7 March 2013.
173. Qian, K.; Edwards, K.E.; Mennito, A.S.; Saeger, R.B. Generation of Model-of-Composition of Petroleum by High Resolution Mass Spectrometry and Associated Analytics. U.S. Patent US20120153139A1, 21 June 2012.
174. Yerabolu, R.; Kotha, R.R.; Niyonsaba, E.; Dong, X.; Manheim, J.M.; Kong, J.; Riedeman, J.S.; Romanczyk, M.; Johnston, C.T.; Kilaz, G.; et al. Molecular profiling of crude oil by using Distillation Precipitation Fractionation Mass Spectrometry (DPF-MS). *Fuel* **2018**, *234*, 492–501. [CrossRef]
175. Manheim, J.; Zhang, Y.; Viidanoja, J.; Kenttämaa, H.I. An Automated Method for Chemical Composition Analysis of Lubricant Base Oils by Using Atmospheric Pressure Chemical Ionization Mass Spectrometry. *J. Am. Soc. Mass Spectrom.* **2019**, *30*, 2014–2021. [CrossRef]
176. Alzarieni, K.Z.; Zhang, Y.; Niyonsaba, E.; Wehde, K.E.; Johnston, C.T.; Kilaz, G.; Kenttämaa, H.I. Determination of the Chemical Compositions of Condensate-like Oils with Different API Gravities by Using the Distillation, Precipitation, Fractionation Mass Spectrometry (DPF MS) Method. *Energy Fuels* **2021**, *35*, 8646–8656. [CrossRef]
177. Zhang, Y.; Schulz, F.; Rytting, B.M.; Walters, C.C.; Kaiser, K.; Metz, J.N.; Harper, M.R.; Merchant, S.S.; Mennito, A.S.; Qian, K.; et al. Elucidating the Geometric Substitution of Petroporphyrins by Spectroscopic Analysis and Atomic Force Microscopy Molecular Imaging. *Energy Fuels.* **2019**, *33*, 6088–6097. [CrossRef]
178. Zhao, X.; Liu, Y.; Xu, C.; Yan, Y.; Zhang, Y.; Zhang, Q.; Zhao, S.; Chung, K.; Gray, M.R.; Shi, Q. Separation and Characterization of Vanadyl Porphyrins in Venezuela Orinoco Heavy Crude Oil. *Energy Fuels* **2013**, *27*, 6, 2874–2882. [CrossRef]
179. Wu, J.; Zhang, W.; Ma, C.; Ren, L.; Li, S.; Zhang, Y.; Shi, Q. Separation and characterization of squalene and carotenoids derived sulfides in a low mature crude oil. *Fuel* **2020**, *270*, 117536. [CrossRef]
180. Covas, T.; Santos de Freitas, C.; Tose, L.; Valencia-Dávila, J.; Rocha, Y.; Rangel, M.; Cabral da Silva, R.; Vaz, B. Fractionation of polar compounds from crude oils by hetero-medium pressure liquid chromatography (H-MPLC) and molecular characterization by ultrahigh-resolution mass spectrometry. *Fuel* **2020**, *267*, 117289. [CrossRef]
181. Zheng, F.; Shi, Q.; Vallverdu, G.S.; Giusti, P.; Bouyssiere, B. Fractionation and Characterization of Petroleum Asphaltene: Focus on Metalopetroleomics. *Processes* **2020**, *8*, 1504. [CrossRef]
182. Hemmingsen, V.; Sunghwan, K.; Pettersen, H.; Rodgers, R.; Sjoblom, J.; Marshall, A. Structural Characterization and Interfacial Behavior of Acidic Compounds Extracted from a North Sea Oil. *Energy Fuels* **2006**, *20*, 1980–1987. [CrossRef]
183. Colati, K.A.; Dalmaschio, G.P.; de Castro, E.V.; Gomes, A.O.; Vaz, B.G.; Romão, W. Monitoring the liquid/liquid extraction of naphthenic acids in brazilian crude oil using electrospray ionization FT-ICR mass spectrometry (ESI FT-ICR MS). *Fuel* **2013**, *108*, 647–655. [CrossRef]
184. Seifert, W.; Howells, W. lnterfacially active acids in a California crude oil. Isolation of carboxylic acids and phenols. *Anal. Chem.* **1969**, *41*, 554–562. [CrossRef]
185. Barros, E.V.; Dias, H.P.; Pinto, F.E.; Gomes, A.O.; Moura, R.R.; Neto, A.C.; Freitas, J.C.C.; Aquije, G.M.F.V.; Vaz, B.G.; Romão, W. Characterization of Naphthenic Acids in Thermally Degraded Petroleum by ESI(−)-FT-ICR MS and ^{1}H NMR after Solid-Phase Extraction and Liquid/Liquid Extraction. *Energy Fuels* **2018**, *32*, 2878–2888. [CrossRef]
186. Fan, T.P. Characterization of naphthenic acids in petroleum by fast atom bombardment mass spectrometry. *Energy Fuels* **1991**, *5*, 371–375. [CrossRef]
187. Dzidic, I.; Somerville, A.C.; Raia, J.C.; Hart, H.V. Determination of naphthenic acids in California crudes and refinery wastewaters by fluoride ion chemical ionization mass spectrometry. *Anal. Chem.* **1988**, *60*, 1318–1323. [CrossRef]
188. Rowland, S.M.; Robbins, W.K.; Corilo, Y.E.; Marshall, A.G.; Rodgers, R.P. Solid-Phase Extraction Fractionation To Extend the Characterization of Naphthenic Acids in Crude Oil by Electrospray Ionization Fourier Transform Ion Cyclotron Resonance Mass Spectrometry. *Energy Fuels* **2014**, *28*, 5043–5048. [CrossRef]
189. Clingenpeel, A.C.; Fredriksen, T.R.; Qian, K.; Harper, M.R. Comprehensive Characterization of Petroleum Acids by Distillation, Solid Phase Extraction Separation, and Fourier Transform Ion Cyclotron Resonance Mass Spectrometry. *Energy Fuels* **2018**, *32*, 9271–9279. [CrossRef]

190. Saab, J.; Mokbel, A.; Razzouk, N.; Zydowicz, N.; Jose, J. Quantitative extraction produce of naphthenic acids contained in crude oils. Characterization with different spectroscopic methods. *Energy Fuels* **2005**, *19*, 525–531. [CrossRef]
191. Barros, E.V.; Souza, L.M.; Madeira, N.C.; Chinelatto, L.S.; Bertelli, J.N.; Carvalho, R.M.; Vaz, B.G.; Simas, R.C.; Neto, A.C.; Lacerda, V.; et al. Isolation of tetrameric acids from naphthenates deposits and characterization by high-resolution analytical techniques. *Fuel* **2021**, *308*, 122065. [CrossRef]
192. Barros, E.; Filgueiras, P.; Lacerda, V., Jr.; Rodgers, R.; Romao, W. Characterization of naphthenic acids in crude oil samples—A literature review. *Fuel* **2022**, *319*, 123775. [CrossRef]
193. Putmann, J.; Marshall, A. Screening petroleum crude oils for ARN tetraprotic acids with molecularly imprinted polymers. *Energy Fuels* **2016**, *30*, 5651–5655. [CrossRef]
194. Andersson, J.T. Separation in the sample preparation for sulfur compound analysis. In *Springer Handbook of Petroleum Technology*; Springer: Cham, Switzerland, 2017; Volume 5, pp. 199–219.
195. Müller, H.; Andersson, J.T.; Schrader, W. Characterization of High-Molecular-Weight Sulfur-Containing Aromatics in Vacuum Residues Using Fourier Transform Ion Cyclotron Resonance Mass Spectrometry. *Anal. Chem.* **2005**, *77*, 2536–2543. [CrossRef]
196. Li, H.; Chen, X.; Wu, J.; Zhang, Y.; Liu, X.; Shi, Q.; Zhao, S.; Xu, C.; Hsu, C.S. Selective Methylation of Sulfides in Petroleum for Electrospray Ionization Mass Spectrometry Analysis. *Energy Fuels* **2019**, *33*, 1797–1802. [CrossRef]
197. Wu, J.; Zhang, W.; Ma, C.; Wang, F.; Zhou, X.; Chung, K.H.; Hou, D.; Zhang, Y.; Shi, Q. Isolation and characterization of sulfur compounds in a lacustrine crude oil. *Fuel* **2019**, *253*, 1482–1489. [CrossRef]
198. Wang, M.; Zhao, S.; Chung, K.H.; Xu, C.; Shi, Q. Approach for Selective Separation of Thiophenic and Sulfidic Sulfur Compounds from Petroleum by Methylation/Demethylation. *Anal. Chem.* **2015**, *87*, 1083–1088. [CrossRef]
199. Qian, K.; Edwards, K.E.; Mennito, A.S.; Walters, C.C.; Kushnerick, J.D. Enrichment, Resolution, and Identification of Nickel Porphyrins in Petroleum Asphaltene by Cyclograph Separation and Atmospheric Pressure Photoionization Fourier Transform Ion Cyclotron Resonance Mass Spectrometry. *Anal. Chem.* **2010**, *82*, 413–419. [CrossRef] [PubMed]
200. Qian, K.; Fredriksen, T.R.; Mennito, A.S.; Zhang, Y.; Harper, M.R.; Merchant, S.; Kushnerick, J.D.; Rytting, B.M.; Kilpatrick, P.K. Evidence of naturally-occurring vanadyl porphyrins containing multiple S and O atoms. *Fuel* **2018**, *239*, 1258–1264. [CrossRef]
201. Rytting, B.M.; Singh, I.D.; Kilpatrick, P.K.; Harper, M.R.; Mennito, A.S.; Zhang, Y. Ultrahigh-Purity Vanadyl Petroporphyrins. *Energy Fuels* **2018**, *32*, 5711–5724. [CrossRef]
202. Pomerantz, A.E.; Mullins, O.C.; Paul, G.; Ruzicka, J.; Sanders, M. Orbitrap Mass Spectrometry: A Proposal for Routine Analysis of Nonvolatile Components of Petroleum. *Energy Fuels* **2011**, *25*, 3077–3082. [CrossRef]
203. McKenna, A.M.; Nelson, R.; Reddy, C.M.; Savory, J.J.; Kaiser, N.K.; Fitzsimmons, J.E.; Marshall, A.G.; Rodgers, R.P. Expansion of the Analytical Window for Oil Spill Characterization by Ultrahigh Resolution Mass Spectrometry: Beyond Gas Chromatography. *Environ. Sci. Technol.* **2013**, *47*, 7530–7539. [CrossRef] [PubMed]
204. Dutriez, T.; Courtiade, M.; Ponthus, J.; Thiébaut, D.; Dulot, H.; Hennion, M.-C. Complementarity of Fourier Transform Ion Cyclotron Resonance Mass Spectrometry and high temperature comprehensive two-dimensional gas chromatography for the characterization of resin fractions from vacuum gas oils. *Fuel* **2012**, *96*, 108–119. [CrossRef]
205. Santos, J.; Wisniewski, A.; Eberlin, M.; Schrader, W. Comparing Crude Oils with Different API Gravities on a Molecular Level Using Mass Spectrometric Analysis. Part 1: Whole Crude Oil. *Energies* **2018**, *11*, 2766. [CrossRef]
206. Santos, J.; Vetere, A.; Wisniewski, A.; Eberlin, M.; Schrader, W. Comparing Crude Oils with Different API Gravities on a Molecular Level Using Mass Spectrometric Analysis. Part 2: Resins and Asphaltenes. *Energies* **2018**, *11*, 2767. [CrossRef]
207. Dalmaschio, G.P.; Malacarne, M.M.; de Almeida, V.M.; Pereira, T.M.; Gomes, A.O.; de Castro, E.V.; Greco, S.J.; Vaz, B.G.; Romão, W. Characterization of polar compounds in a true boiling point distillation system using electrospray ionization FT-ICR mass spectrometry. *Fuel* **2014**, *115*, 190–202. [CrossRef]
208. Wang, Q.; Hao, F.; Cao, Z.; Tian, J. Heteroatom compounds in oils from the Shuntuoguole low uplift, Tarim Basin characterized by (+ESI) FT-ICR MS: Implications for ultra-deep petroleum charges and alteration. *Mar. Pet. Geol.* **2021**, *134*, 105321. [CrossRef]
209. Vaz, B.G.; Silva, R.C.; Klitzke, C.F.; Simas, R.C.; Lopes Nascimento, H.D.; Pereira, R.C.; Garcia, D.F.; Eberlin, M.N.; Azevedo, D.A. Assessing Biodegradation in the Llanos Orientales Crude Oils by Electrospray Ionization Ultrahigh Resolution and Accuracy Fourier Transform Mass Spectrometry and Chemometric Analysis. *Energy Fuels* **2013**, *27*, 1277–1284. [CrossRef]
210. Krajewski, L.C.; Rodgers, R.P.; Marshall, A.G. 126 264 Assigned Chemical Formulas from an Atmospheric Pressure Photoionization 9.4 T Fourier Transform Positive Ion Cyclotron Resonance Mass Spectrum. *Anal. Chem.* **2017**, *89*, 11318–11324. [CrossRef] [PubMed]
211. Handle, F.; Harir, M.; Füssl, J.; Koyun, A.N.; Grossegger, D.; Hertkorn, N.; Eberhardsteiner, L.; Hofko, B.; Hospodka, M.; Blab, R.; et al. Tracking Aging of Bitumen and Its Saturate, Aromatic, Resin, and Asphaltene Fractions Using High-Field Fourier Transform Ion Cyclotron Resonance Mass Spectrometry. *Energy Fuels* **2017**, *31*, 4771–4779. [CrossRef]
212. Martins, L.L.; Pudenzi, M.A.; da Cruz, G.F.; Nascimento, H.D.L.; Eberlin, M.N. Assessing Biodegradation of Brazilian Crude Oils via Characteristic Profiles of O_1 and O_2 Compound Classes: Petroleomics by Negative-Ion Mode Electrospray Ionization Fourier Transform Ion Cyclotron Resonance Mass Spectrometry. *Energy Fuels* **2017**, *31*, 6649–6657. [CrossRef]
213. Cho, Y.; Birdwell, J.E.; Hur, M.; Lee, J.; Kim, B.; Kim, S. Extension of the Analytical Window for Characterizing Aromatic Compounds in Oils Using a Comprehensive Suite of High-Resolution Mass Spectrometry Techniques and Double Bond Equivalence versus Carbon Number Plot. *Energy Fuels* **2017**, *31*, 7874–7883. [CrossRef]

214. Kostyukevich, Y.I.; Zherebker, A.Y.; Vlaskin, M.S.; Borisova, L.; Nikolaev, E.N. Microprobe for the Thermal Analysis of Crude Oil Coupled to Photoionization Fourier Transform Mass Spectrometry. *Anal. Chem.* **2018**, *90*, 8756–8763. [CrossRef]
215. Schmidt, E.M.; Pudenzi, M.A.; Santos, J.M.; Angolini, C.F.F.; Pereira, R.C.L.; Rocha, Y.S.; Denisov, E.; Damoc, E.; Makarov, A.; Eberlin, M.N. Petroleomics via Orbitrap Mass Spectrometry with Resolving Power above 1 000 000 at m/z 200. *RSC Adv.* **2018**, *8*, 6183–6191. [CrossRef]
216. Yalaoui-Guellal, D.; Temzi, S.; Dib, S.; KumarSahu, S.; Irorere, U.V.; Banat, I.; Madani, K. The petroleum-degrading bacteria Alcaligenes aquatilis strain YGD 2906 as a potential source of lipopeptide biosurfactant. *Fuel* **2021**, *285*, 119112. [CrossRef]
217. Zhang, W.; Andersson, J.; JoachimRäder, H.; Müllen, K. Molecular characterization of large polycyclic aromatic hydrocarbons in solid petroleum pitch and coal tar pitch by high resolution MALDI ToF MS and insights from ion mobility separation. *Carbon* **2015**, *95*, 672–680. [CrossRef]
218. Cho, Y.; Ahmed, A.; Islam, A.; Kim, S. Developments in FT-ICR MS Instrumentation, Ionization Techniques, and Data Interpretation Methods for Petroleomics. *Mass Spectrom. Rev.* **2015**, *34*, 248–263. [CrossRef]
219. Wu, Z.; Rodgers, R.P.; Marshall, A.G.; Strohm, J.J.; Song, C. Comparative Compositional Analysis of Untreated and Hydrotreated Oil by Electrospray Ionization Fourier Transform Ion Cyclotron Resonance Mass Spectrometry. *Energy Fuels* **2005**, *19*, 1072–1077. [CrossRef]
220. Hughey, C.; Rodgers, R.P.; Marshall, A.G.; Qian, K.; Robbins, W.K. Identification of acidic NSO compounds in crude oils of different geochemical origins by negative ion electrospray Fourier transform ion cyclotron resonance mass spectrometry. *Org. Geochem.* **2002**, *33*, 743–759. [CrossRef]
221. A Hughey, C.; Rodgers, R.P.; Marshall, A.G.; Walters, C.C.; Qian, K.; Mankiewicz, P. Acidic and neutral polar NSO compounds in Smackover oils of different thermal maturity revealed by electrospray high field Fourier transform ion cyclotron resonance mass spectrometry. *Org. Geochem.* **2004**, *35*, 863–880. [CrossRef]
222. Guricza, L.M.; Schrader, W. Electrospray ionization for determination of non-polar polyaromatic hydrocarbons and polyaromatic heterocycles in heavy crude oil asphaltenes. *Biol. Mass Spectrom.* **2015**, *50*, 549–557. [CrossRef] [PubMed]
223. Kim, Y.H.; Kim, S. Improved abundance sensitivity of molecular ions in positive-ion APCI MS analysis of petroleum in toluene. *J. Am. Soc. Mass Spectrom.* **2010**, *21*, 386–392. [CrossRef]
224. Pereira, T.M.C.; Vanini, G.; Oliveira, E.C.S.; Cardoso, F.M.R.; Fleming, F.P.; Neto, A.C.; Lacerda, V., Jr.; Castro, E.V.R.; Vaz, B.G.; Romão, W. An evaluation of the aromaticity of asphaltenes using atmospheric pressure photoionization Fourier transform ion cyclotron resonance mass spectrometry—APPI(±) FT-ICRMS. *Fuel* **2014**, *118*, 348–357. [CrossRef]
225. Schrader, W.; Panda, S.K.; Brockmann, K.J.; Benter, T. Characterization of non-polar aromatic hydrocarbons in crude oil using atmospheric pressure laser ionization and Fourier transform ion cyclotron resonance mass spectrometry (APLI FT-ICR MS). *Anallyst* **2008**, *133*, 867–869. [CrossRef]
226. Palacio Lozano, D.C.; Orrego-Ruiz, J.A.; Barrow, M.P.; Cabanzo Hernandez, R.; Mejía-Ospino, E. Analysis of the molecular weight distribution of vacuum residues and their molecular distillation fractions by laser desorption ionization mass spectrometry. *Fuel* **2016**, *171*, 247–252. [CrossRef]
227. Vanini, G.; Barra, T.A.; Souza, L.M.; Madeira, N.C.; Gomes, A.O.; Romão, W.; Azevedo, D.A. Characterization of nonvolatile polar compounds from Brazilian oils by electrospray ionization with FT-ICR MS and Orbitrap-MS. *Fuel* **2020**, *282*, 118790. [CrossRef]
228. Hourani, N.; Muller, H.; Adam, F.M.; Panda, S.K.; Witt, M.; Al-Hajji, A.A.; Sarathy, S.M. Structural Level Characterization of Base Oils Using Advanced Analytical Techniques. *Energy Fuels* **2015**, *29*, 2962–2970. [CrossRef]
229. Klesper, G.; Röllgen, F. Field-induced Ion Chemistry Leading to the Formation of (M-2nH)+· and (2M-2mH)+· Ions in Field Desorption Mass Spectrometry of Saturated Hydrocarbons. *J. Mass Spectrom.* **1996**, *31*, 383–388. [CrossRef]
230. Qian, K.; Dechert, G.J. Recent Advances in Petroleum Characterization by GC Field Ionization Timeof-Flight High-Resolution Mass Spectrometry. *Anal. Chem.* **2002**, *74*, 3977–3983. [CrossRef]
231. Vozka, P.; Mo, H.; Šimáček, P.; Kilaz, G. Middle distillates hydrogen content via GC×GC-FID. *Talanta* **2018**, *186*, 140–146. [CrossRef] [PubMed]
232. Alexandrino, G.L.; de Sousa, G.R.; de A., M. Reis, F.; Augusto, F. Optimizing Loop-Type Cryogenic Modulation in Comprehensive Two-Dimensional Gas Chromatography Using Time-Variable Combination of the Dual-Stage Jets for Analysis of Crude Oil. *J. Chromatogr. A* **2018**, *1536*, 82–87. [CrossRef] [PubMed]
233. Potgieter, H.; Bekker, R.; Beigley, J.; Rohwer, E. Analysis of oxidised heavy paraffininc products by high temperature comprehensive two-dimensional gas chromatography. *J. Chromatogr. A* **2017**, *1509*, 123–131. [CrossRef] [PubMed]
234. Rowland, S.J.; West, C.E.; Scarlett, A.; Jones, D. Identification of individual acids in a commercial sample of naphthenic acids from petroleum by two-dimensional comprehensive gas chromatography/mass spectrometry. *Rapid Commun. Mass Spectrom.* **2011**, *25*, 1741–1751. [CrossRef]
235. Jennerwein, M.K.; Eschner, M.S.; Wilharm, T.; Zimmermann, R.; Gröger, T.M. Proof of Concept of High-Temperature Comprehensive Two-Dimensional Gas Chromatography Time-of-Flight Mass Spectrometry for Two-Dimensional Simulated Distillation of Crude Oils. *Energy Fuels* **2017**, *31*, 11651–11659. [CrossRef]
236. Byer, J.D.; Siek, K.; Jobst, K. Distinguishing the C3 vs SH4 Mass Split by Comprehensive Two-Dimensional Gas Chromatography–High Resolution Time-of-Flight Mass Spectrometry. *Anal. Chem.* **2016**, *88*, 6101–6104. [CrossRef]
237. Vanini, G.; Pereira, V.B.; Romão, W.; Gomes, A.O.; Oliveira, L.M.S.; Dias, J.C.M.; Azevedo, D.A. Analytical advanced techniques in the molecular-level characterization of Brazilian crude oils. *Microchem. J.* **2018**, *137*, 111–118. [CrossRef]

238. Kim, D.; Jin, J.M.; Cho, Y.; Kim, E.-H.; Cheong, H.-K.; Kim, Y.H.; Kim, S. Combination of ring type HPLC separation, ultrahigh-resolution mass spectrometry, and high field NMR for comprehensive characterization of crude oil compositions. *Fuel* **2017**, *157*, 48–55. [CrossRef]
239. Rivera-Barrera, D.; Rueda-Chacón, H.; Molina, M. Prediction of the total acid number (TAN) of colombian crude oils via ATR–FTIR spectroscopy and chemometric methods. *Talanta* **2019**, *206*, 120186. [CrossRef] [PubMed]
240. Folli, G.S.; Nascimento, M.H.; De Paulo, E.H.; Da Cunha, P.H.; Romão, W.; Filgueiras, P.R. Variable selection in support vector regression using angular search algorithm and variance inflation factor. *J. Chemom.* **2020**, *34*, e3282. [CrossRef]
241. Mohammadi, M.; Khorrami, M.K.; Hamid Vatanparast, H.; Karimi, A.; Sadrara, M. Classification and determination of sulfur content in crude oil samples by infrared spectrometry. *Infrared Phys. Technol.* **2022**, *127*, 104382. [CrossRef]
242. Filgueiras, P.R.; Sad, C.M.; Loureiro, A.R.; Santos, M.F.; Castro, E.V.; Dias, J.C.; Poppi, R.J. Determination of API gravity, kinematic viscosity and water content in petroleum by ATR-FTIR spectroscopy and multivariate calibration. *Fuel* **2014**, *116*, 123–130. [CrossRef]
243. Dearing, T.I.; Thompson, W.J.; Rechsteiner, C.E.; Marquardt, B.J. Characterization of Crude Oil Products Using Data Fusion of Process Raman, Infrared, and Nuclear Magnetic Resonance (NMR) Spectra. *Appl. Spectrosc.* **2011**, *65*, 181–186. [CrossRef]
244. Falla, F.; Larini, C.; Le Roux, G.; Quina, F.; Moro, L.; Nascimento, C. Characterization of crude petroleum by NIR. *J. Pet. Sci. Eng.* **2006**, *51*, 127–137. [CrossRef]
245. Mohammadi, M.; Khorrami, M.K.; Vatani, A.; Ghasemzadeh, H.; Vatanparast, H.; Bahramian, A.; Fallah, A. Rapid determination and classification of crude oils by ATR-FTIR spectroscopy and chemometric methods. *Spectrochim. Acta Part A Mol. Biomol. Spectrosc.* **2020**, *232*, 118157. [CrossRef]
246. Brakstad, F.; Karstang, T.V.; Sørensen, J.; Steen, A. Prediction of molecular weight and density of distillation fractions from gas chromatographic—Mass spectrometric detection and multivariate calibration. *Chemom. Intell. Lab. Syst.* **1988**, *3*, 321–328. [CrossRef]
247. Melendez, L.; Lache, A.; Ruiz, O.; Pacho, Z.; Ospino, E.M. Prediction of the SARA analysis of Colombian crude oils using ATR–FTIR spectroscopy and chemometric methods. *J. Pet. Sci. Eng* **2012**, *90–91*, 56–60. [CrossRef]
248. Rodrigues, R.R.; Rocha, J.T.; Oliveira, L.M.S.; Dias, J.C.M.; Müller, E.I.; Castro, E.V.; Filgueiras, P.R. Evaluation of calibration transfer methods using the ATR-FTIR technique to predict density of crude oil. *Chemom. Intell. Lab. Syst.* **2017**, *166*, 7–13. [CrossRef]
249. Rainha, K.P.; Rocha, J.T.D.C.; Rodrigues, R.R.T.; Lovatti, B.P.D.O.; De Castro, E.V.R.; Filgueiras, P.R. Determination of API Gravity and Total and Basic Nitrogen Content by Mid- and Near-Infrared Spectroscopy in Crude Oil with Multivariate Regression and Variable Selection Tools. *Anal. Lett.* **2019**, *52*, 2914–2930. [CrossRef]
250. Flumignan, D.L.; de Oliveira Ferreira, F.; Tininis, A.G.; de Oliveira, J.E. Multivariate calibrations in gas chromatographic profiles for prediction of several physicochemical parameters of Brazilian commercial gasoline. *Chemometr. Intell. Lab.* **2008**, *92*, 53–60. [CrossRef]
251. Long, J.; Wang, K.; Yang, M.; Zhong, W. Rapid crude oil analysis using near-infrared reflectance spectroscopy. *Pet. Sci. Technol.* **2018**, *37*, 354–360. [CrossRef]
252. Moro, M.K.; Neto, A.C.; Lacerda, V.; Romão, W.; Chinelatto, L.S.; Castro, E.V.; Filgueiras, P.R. FTIR, 1H and 13C NMR data fusion to predict crude oils properties. *Fuel* **2019**, *263*, 116721. [CrossRef]